

1    **A model screening pipeline for bile acid converting anti-*Clostridioides***  
2    ***difficile* bacteria reveals unique biotherapeutic potential of**  
3    ***Peptacetobacter hiranonis***

4    Akhil A. Vinithakumari<sup>a</sup>, Belen G. Hernandez<sup>a</sup>, Sudeep Ghimire<sup>e</sup>, Seidu  
5    Adams<sup>e</sup>, Caroline Stokes<sup>a</sup>, Isaac Jepsen<sup>a</sup>, Caleb Brezina<sup>a</sup>, Orhan Sahin<sup>c</sup>,  
6    Ganwu Li<sup>c</sup>, Chandra Tangudu<sup>b</sup>, Claire Andreasen<sup>a</sup>, Gregory J. Philips<sup>b</sup>,  
7    Michael Wannemuehler<sup>b</sup>, Albert E. Jergens<sup>d</sup>, Joy Scaria<sup>e</sup>, Brett Sponseller<sup>b</sup>,  
8    and Shankumar Mooyottu <sup>a\*</sup>

9    <sup>a</sup>*Department of Veterinary Pathology, Iowa State University, Ames, IA, USA*

10    <sup>b</sup>*Department of Veterinary Microbiology and Preventive Medicine, Iowa State*  
11    *University, Ames, IA, USA*

12    <sup>c</sup>*Department of Veterinary Diagnostic and Production Animal Medicine, Iowa State*  
13    *University, Ames, IA, USA*

14    <sup>d</sup>*Department of Veterinary Clinical Sciences, Iowa State University, Ames, IA, USA*

15    <sup>e</sup>*Department of Veterinary & Biomedical Sciences, South Dakota State University,*  
16    *Brookings, SD, USA*

17    \*Corresponding author:

18    Shankumar Mooyottu

19    [shaan@iastate.edu](mailto:shaan@iastate.edu)

20    515-294-3877

21

## 22 Abstract

23 *Clostridoides difficile* is an antibiotic-resistant bacterium that causes serious, toxin-mediated  
24 enteric disease in humans and animals. Gut dysbiosis and resultant alterations in the intestinal bile  
25 acid profile play an important role in the pathogenesis of *C. difficile* infection (CDI). Restoration  
26 of the gut microbiota and re-establishment of bacterial bile acid metabolism using fecal microbiota  
27 transplantation (FMT) has been established as a promising strategy against this disease, although  
28 this method has several limitations. Thus, a more defined and precise microbiota-based approach  
29 using bacteria that biotransform primary bile acids into secondary bile acids could effectively  
30 overcome these limitations and control CDI. Therefore, a screening pipeline was developed to  
31 isolate bile acid converting bacteria from fecal samples. Dogs were selected as a model CDI-  
32 resistant microbiota donor for this pipeline, which yielded a novel *Peptacetobacter hiranonis*  
33 strain that possesses unique anti-*C. difficile* properties, and both bile acid deconjugation and 7- $\alpha$   
34 dehydroxylating activities to perform bile acid conversion. The screening pipeline included a set  
35 of *in vitro* tests along with a precision *in vivo* gut colonization and bile acid conversion test using  
36 altered Schadler flora (ASF) colonized mice. In addition, this pipeline also provided essential  
37 information on the growth requirements for screening and cultivating the candidate bacterium, its  
38 survival in a CDI predisposing environment, and potential pathogenicity. The model pipeline  
39 documented here yielded multiple bile acid converting bacteria, including a *P. hiranonis* isolate  
40 with unique anti-*C. difficile* biotherapeutic potential, which can be further tested in subsequent  
41 preclinical and human clinical trials.

42 **Keywords:** *Peptacetobacter hiranonis*, bile acid, *C. difficile* infection, ASF mice, *bai*-operon

43 **Introduction**

44 *Clostridioides difficile* infection (CDI) is a serious toxin-mediated enteric disease  
45 affecting humans and animals.<sup>1-3</sup> Antibiotic therapy, gut-dysbiosis, and resultant  
46 alterations in the intestinal bile acid profile play important roles in CDI disease  
47 pathogenesis.<sup>1,4</sup> Annually, approximately half a million people in the United States suffer  
48 from CDI, which incurs approximately \$5 billion in treatment and prevention costs.<sup>5</sup>  
49 Recent studies indicate that 1 out of every 11 patients aged 65 or older dies within 30  
50 days of CDI diagnosis.<sup>6</sup> *C difficile* is also a significant animal pathogen that causes serious  
51 enteric disease, mortality, and economic losses in a variety of species, especially in pigs  
52 with the potential for zoonotic transmission.<sup>7,8</sup> Currently, antibiotics are the primary  
53 treatment for CDI despite the risk of further aggravation of dysbiosis, relapse of infection,  
54 and development of antibiotic resistance.<sup>9</sup> Recently, *C. difficile* has been listed as an  
55 urgent threat by the Center for Disease Control and Prevention (CDC) concerning the  
56 emergence of antibiotic resistance.<sup>10</sup> Therefore, the development of an effective,  
57 alternative approach for controlling CDI is critical. Restoration of the gut microbiome  
58 and re-establishment of normal bile acid metabolism using fecal microbiota  
59 transplantation (FMT) has been recently established as a promising and effective strategy  
60 against this disease.<sup>11-13</sup> Unfortunately, the concerns of transmission of bacterial and viral  
61 pathogens and reports of deaths associated with FMT highlight the need for more defined  
62 and precise microbiome-based approaches for controlling CDI in patients.<sup>14,15</sup>

63 The liver primarily synthesizes cholic acid (CA) and chenodeoxycholic acid  
64 (CDCA) from cholesterol in hepatocytes. Therefore, CA and CDCA are known as  
65 primary bile acids that are conjugated with glycine or taurine to form conjugated primary  
66 bile acids (e.g., taurocholic acid (TCA)), which are secreted into the small intestine.<sup>16,17</sup>  
67 In mice, muricholic acid (MCA) is also synthesized in the liver along with CA and CDCA

68 as a primary bile acid.<sup>18</sup> Several bile salt hydrolyzing gut bacteria that contain the *bsh*  
69 (bile salt hydrolase) gene deconjugate secreted primary bile acids.<sup>17</sup> At the same time, a  
70 few species of 7- $\alpha$  dehydroxylating bacteria, such as *Clostridium scindens* and  
71 *Peptacetobacter hiranonis* (previously *Clostridium hiranonis*), that contain the crucial  
72 *bai* operon (bile acid-inducible operon), convert these deconjugated primary bile acids  
73 into secondary bile acids including deoxycholic acid (DCA) and lithocholic acid  
74 (LCA).<sup>16, 17</sup> Primary bile acid CA facilitates the germination of *C. difficile* spores, whereas  
75 secondary bile acids, formed by bacterial conversion of the primary bile acids in the colon  
76 strongly inhibit the growth of *C. difficile* in the host.<sup>19-21</sup> In addition, bile acids directly  
77 bind and inhibit the activity of *C. difficile* toxin in the gut and modulate host immune and  
78 inflammatory responses.<sup>13, 22, 23</sup> Long-term antibiotic therapy with resultant dysbiosis in  
79 humans precipitate CDI by eliminating bile acid converting bacteria (both *bsh* and *bai*  
80 containing species) in the intestine, increasing the available primary bile acids, and  
81 reducing the pool of secondary bile acids.<sup>4</sup> Therefore, bile acid metabolizing bacteria,  
82 especially rare *bai* containing species have immense therapeutic value for the treatment  
83 of CDI.<sup>19</sup> As opposed to the current strategy of providing a whole fecal microbiota  
84 mixture (FMT) to the patient, a targeted and' precision microbiome'-based strategy for  
85 normalizing the gut bile acid profile has been proposed as a promising alternative for  
86 controlling CDI.<sup>19, 24</sup> Therefore, there is a critical need to identify and isolate *bai* coding  
87 bacterial strains and to demonstrate the bile-acid converting ability to exploit their  
88 prophylactic and therapeutic potential. These bacteria have immense potential to be used  
89 as live biotherapeutic agents to prevent and treat CDI as a functional alternative to  
90 antibiotics and conventional FMT or to formulate an enriched or defined FMT  
91 preparation.

92 The presence of bile acid metabolizing bacteria such as *C. scindens* and *P.*  
93 *hiranonis* in the resident gut microbiota is associated with notable resistance to *C. difficile*  
94 colonization in different mammalian hosts, especially in dogs.<sup>20,25</sup> However, identifying,  
95 isolating, and cultivating these unique, invaluable, but fastidious anaerobes is  
96 challenging. Therefore, only few isolates of *C. scindens* and virtually none of *P. hiranonis*  
97 have been fully characterized in the laboratory for growth conditions, *in vitro* and *in vivo*  
98 bile acid conversion ability, gut colonization, and anti-*C. difficile* therapeutic properties.

99 In this study, a model pipeline is described for isolating bile acid converting  
100 bacteria, such as *P. hiranonis*, from naturally *C. difficile* resistant hosts. The model takes  
101 advantage of dogs as a model host naturally resistant to CDI. This approach involves a  
102 series of *in vitro* tests and a novel *in vivo* gut colonization and bile acid conversion model  
103 using Altered Schadler Flora (ASF) colonized mice. In addition, this pipeline also  
104 provides essential information on the growth requirements of the candidate bacterium  
105 (e.g., *P. hiranonis*), its survival in a CDI predisposing gut environment, enterotoxicity,  
106 and *in vivo* and *in vitro* bile acid converting abilities. These data are critical for further  
107 preclinical infection studies and clinical trials. Thus, this manuscript documents the steps  
108 involved in this pipeline that resulted in the identification and characterization of a unique  
109 *P. hiranonis* isolate (*P. hiranonis BAI-17*) with anti-*C. difficile* therapeutic value.  
110 Additionally, this study establishes *P. hiranonis* as the only bacterium currently known  
111 to have both bile acid hydrolyzing and 7- $\alpha$  hydroxylation capabilities, which are  
112 demonstrated *in vitro* and *in vivo*. The unique combination of functional *bai* and *bsh* genes  
113 within a single bacterial genome makes *P. hiranonis* a promising biotherapeutic candidate  
114 for targeted microbiome-based therapy against CDI in humans and animals.

115 **Results**

116 **Specific *P. hiranonis* strains and other anaerobes from canine feces are**  
117 **selectively isolated in a beta-lactam -fluoroquinolone-bile acid environment**

118 For this study, dogs were selected as the model *C. difficile* resistant donors due to  
119 their natural resistance to CDI, which is attributed to the abundance of bile acid converting  
120 bacteria such as *P. hiranonis* in the canine gut.<sup>25</sup> To isolate *bai*-containing bacteria with  
121 anti-*C. difficile* properties, we screened dog fecal samples in Taurocholate Moxalactam  
122 Norfloxacin Fructose medium (TMNF). TMNF is a modified version of *Clostridium*  
123 *difficile* Moxalactam Norfloxacin (CDMN) medium, a less commonly used medium for  
124 isolating *C. difficile* from fecal and other complex biological and environmental  
125 samples.<sup>26,27</sup> TMNF was used since an ideal anti-*C. difficile* bacterium should survive the  
126 same antibiotic pressure that commonly predisposes CDI in human patients, i.e.  
127 dysbiosis-inducing beta-lactams and fluoroquinolones.<sup>28</sup> Thus, the isolated bacterium  
128 could serve as an adjunct live therapeutic along with dysbiosis-inducing antibiotics to  
129 prevent CDI. Therefore, screening donor fecal samples in a beta-lactam (Moxalactam)  
130 and fluoroquinolone (Norfloxacin) containing medium (TMNF) could provide a selective  
131 advantage for the candidate bacterial strains screened in this isolation process. In addition,  
132 the primary bile acid TCA in the medium could favor the isolation of bile acid  
133 metabolizing bacteria from donor samples. For the current study, further selection of  
134 presumptive colonies on TMNF agar was based on proline aminopeptidase activity, a  
135 quick disc-based test with a special emphasis on *P. hiranonis*. Proline aminopeptidase  
136 positive bacteria of interest include the *bai*-containing species- *P. hiranonis*, *C.*  
137 *bif fermentans*, *C. sordellii* and the pathogen, *C. difficile*.<sup>29</sup>

138 The TMNF screening method effectively yielded five bacterial isolates from 50  
139 samples tested known to have *bai*-operon (10% isolation rate), including two isolates of  
140 *C. bif fermentans*, two isolates of *P. hiranonis*, and one isolate of *C. sordellii*. As expected,  
141 this screening method also yielded three *C. difficile* isolates (6% prevalence) (**Table 1**).  
142 In parallel, the canine fecal samples were screened in Cycloserine Cefoxitin Fructose  
143 Agar (CCFA), a widely used *C. difficile* isolation medium. The isolation rate for *bai*-  
144 operon containing bacteria was 4.77% (isolates of *C. sordelli* and *C. bif fermentans*, and  
145 no *P. hiranonis*) with this isolation method, even after an extended screening of 270 dog  
146 fecal samples using this medium (**supplementary table 1**). However, recovery of *C.*  
147 *difficile* was higher (23%) in this method. Out of five isolates of *bai*-containing bacteria  
148 recovered from TMNF medium, the data from a unique *P. hiranonis* isolate (named *P.*  
149 *hiranonis BAI-17*) with notable anti-*C. difficile* biotherapeutic potential is presented in  
150 detail in this manuscript to describe the additional steps involved in our screening  
151 pipeline.

152 Phenotypically, *P. hiranonis BAI-17* formed irregular translucent to rough grey  
153 colonies with serrated edges, very similar to *C. difficile* on blood agar plates. As  
154 previously mentioned, the proline aminopeptidase test is considered a rapid test for *C.*  
155 *difficile* does not distinguish *P. hiranonis* from *C. difficile*.<sup>30</sup> The lack of fluorescence  
156 under UV light is found to be an easy test that differentiated *P. hiranonis BAI-17* from *C.*  
157 *difficile* (**Supplementary figure 1**).

158 ***P. hiranonis BAI-17 possesses a unique combination of both *bsh* and *bai* genes***  
159 ***with the absence of known toxin genes***

160 An initial Illumina MiSeq-based whole-genome shotgun (WGS)  
161 sequencing of *P. hiranonis BAI-17* confirmed the presence of the *bai* operon and other  
162 bile acid metabolism-related genes. The annotation of the contigs by Rapid Annotation

163 using Subsystem Technology (RAST) and mapping against *P. hiranonis* DSM 13275 in  
164 Geneious Prime software (Biomatters Inc, San Diego, CA) revealed both the presence of  
165 a unique *bai* operon involved in primary bile acid to secondary bile acid conversion (7- $\alpha$   
166 dehydroxylation) and the *bsh* gene (choloylglycine hydrolase), which is responsible for  
167 the hydrolysis of conjugated bile acids required prior to 7- $\alpha$  dihydroxylation (**Figure 2**).  
168 This observation is remarkable because no other gut bacteria (especially Clostridiales)  
169 are known to have both critical genes of bile acid metabolism in a single genome.<sup>31-33</sup>  
170 Further analysis of the currently available *P. hiranonis* genome sequences (one each of  
171 human and dog origin) in GenBank resulted in the same observation of *bai* and *bsh*  
172 presence in those strains.<sup>29, 34</sup>

173 Having both *bsh* gene and *bai* operon in a single bacterium has immense  
174 therapeutic significance. Such bacteria could perform the functions of two different  
175 groups of metabolically dependant commensal bacteria in a dysbiotic gut of a CDI patient  
176 to restore normal bile acid metabolism. Thus, this bacterium alone could be supplemented  
177 as an adjunct prophylactic treatment during the administration of beta-lactams and  
178 fluoroquinolones in susceptible patients or could be administrated as a replacement or  
179 enrichment for FMT.

180 The WGS results also confirmed the presence of genes associated with beta-  
181 lactam and fluoroquinolone resistance in *P. hiranonis* BAI-17 derived from the screening  
182 process (**Figure 3 and supplemental sequence data**). In addition, the intestinal  
183 colonization factor- fibronectin binding protein (FBP) was also identified within the *P.*  
184 *hiranonis* BAI-17 genome. No known toxins or other virulence factors were identified,  
185 suggesting that this bacterium is presumptively non-pathogenic.

186 ***P. hiranonis* is closely related to the bile acid converting gut bacterial species -**

187 ***C. scindens* and *C. hylemonae***

188 The whole-genome shotgun sequencing step included in the screening method  
189 putatively examines the presence of *bai*, *bsh*, and other virulence and antibiotic  
190 resistance-related attributes in the candidate bacterium. However, as an optional step, a  
191 complete genome sequencing of *P. hiranonis* BAI-17 was performed. The hybrid  
192 assembly using Illumina and Nanopore sequencing generated a single contig composed  
193 of 2,511,424 bp. The annotation of the genome using Prokka produced 2,307 total genes  
194 and 2,185 coding sequences. This is comparable to the only other publicly available *C.*  
195 *hiranonis* DSM 13275 genome composed of 2,521,899 bp, which has 2,363 genes and  
196 2,239 CDS, respectively.<sup>32</sup> A circular genome graph of *P. hiranonis* BAI-17 with  
197 complete genome features is given in **Figure 3**.

198 ***Comparative Phylogenomic Analysis of P. hiranonis BAI-17***

199 The comparative phylogenomic analysis of *P. hiranonis* BAI-17, *P. hiranonis*  
200 *DSM 13275*, *C. scindens*, and *C. hylemonae* strains are showed in **Figure 4A**. As shown  
201 in **Figure 5A**, this analysis formed two major clades. *P. hiranonis* BAI-17, *P. hiranonis*  
202 *DSM 13275* and *C. hylemonae* strains clustered together, whereas *C. scindens*  
203 *ATCC35704* and *C. hylemonae* *DSM15053* were the closest species to *P. hiranonis* BAI-  
204 17.

205 ***Pangenome analysis***

206 A pangenome analysis was performed using the following 14 bile degrading bacterial  
207 strains: *P. hiranonis* BAI-17, *P. hiranonis* DSM 13275, *Clostridium scindens*  
208 *BL389WT3D*, *Clostridium scindens* *VE202-05*, *Clostridium scindens* *MSK.1.26*,  
209 *Clostridium scindens* *BL-398-WT-3D*, *Clostridium scindens* *MGYG-HGUT-01303*,  
210 *Clostridium scindens* *MSK.1.16*, *Clostridium scindens* *ATCC35704*, *Clostridium*

211 *hylemonae* MGYG-HGUT-01710, *Clostridium hylemonae* DSM15053, *Clostridium*  
212 *hylemonae* DSM-15053, *Clostridium hylemonae* BSD2780061688st1\_A6, and  
213 *Clostridium hylemonae* BSD2780061688b-171218\_A6. As expected, *P. hiranonis* BAI-  
214 17 clustered with the publicly available human *P. hiranonis* DSM 13275 and formed a  
215 clade with the *C. hylemonae* strains (**Figure 4A**). Also, all *C. scindens* strains clustered  
216 together, forming one clade. The attached bar plot (**Figure 4A**) shows that the average  
217 nucleotide identity (ANI) of the strains clustered according to the species-level variation.  
218 Comparatively, the lowest GC-content was recorded in *P. hiranonis* BAI-17 (0.3125) and  
219 *P. hiranonis* DSM 13275 (0.3128) with the highest percentage completion (100) for both  
220 *P. hiranonis* BAI-17 and *P. hiranonis* DSM 13275. In contrast, the highest GC-content  
221 was registered by the *C. hylemonae* strains (0.4895). There are approximately 2,205 genes  
222 observed in *P. hiranonis* BAI-17 with an average gene length of 955.48. For comparison,  
223 the human *P. hiranonis* DSM 13275 has approximately 2,246 genes with an average gene  
224 length of 941.50. Additionally, the average number of genes observed in *C. scindens* and  
225 *C. hylemonae* strains were 3673.86 and 3565.2, with an average gene length of 875.78  
226 and 981.85, respectively. *P. hiranonis* DSM 13275 has 2,122 gene clusters, which is  
227 higher than *P. hiranonis* BAI17 having 2,105 gene clusters. However, the number of gene  
228 clusters for *P. hiranonis* DSM 13275 was not higher than the average number of gene  
229 clusters in *C. scindens* (3401.26) and *C. hylemonae* (3416) strains. Out of this, 319 and  
230 340 singleton gene clusters were observed in *C. hiranonis* BAI17 and *C. hiranonis* DSM  
231 13275 respectively. The lowest average number of singleton gene clusters were recorded  
232 in *C. scindens* (81.71) and *C. hylemonae* (10.6).

233 **Genome diversity within human and canine *P. hiranonis* strains**

234 Since members of the genus *Peptacetobacter* have highly divergent genomes, the  
235 genome of canine *P. hiranonis* BAI-17 was compared to the human *P. hiranonis* DSM

236 13275 to determine the diversity between *P. hiranonis* species. This analysis  
237 demonstrated that approximately 50,788 genes or gene families were unique to *P.*  
238 *hiranonis BAI-17*, while 51,123 gene families were unique to *P. hiranonis* DSM 13275.  
239 Approximately 1045 gene families were shared between our *P. hiranonis BAI-17* and *P.*  
240 *hiranonis DSM 13275* (**Figure 5A**).

241 In addition, the genomes of *P. hiranonis BAI-17*, *P. hiranonis* DSM 13275, *C.*  
242 *hylemonae MGYG-HGUT-01710*, and *C. scindens* VE20205 were compared. Results  
243 indicated that, 51,063 gene families were unique to *P. hiranonis* DSM13275, 50,723 gene  
244 families were unique to *P. hiranonis BAI-17*, 77,001 gene families were unique to *C.*  
245 *hylemonae MGYG-HGUT-01710* and 82,601 gene families were unique to *C. scindens*  
246 VE20205. Approximately 677 core genes (gene families common to all four strains)  
247 (**Figure 5B**).

248 **Phenotype microarrays provide *P. hiranonis* growth requirements and**  
249 **substrate utilization profile of therapeutic importance**

250 Phenotype microarrays (PM) are one of the most comprehensive microbial cell  
251 metabolic profiling techniques available.<sup>35</sup> Biolog Phenotype Microarray metabolic  
252 panels (PMs 1–8) are composed of 200 assays of carbon source metabolism, 400 assays  
253 of nitrogen source metabolism, 100 assays of phosphorus and sulfur source metabolism,  
254 and 100 assays of other biosynthetic pathways.<sup>35</sup> We performed PM was performed on *P.*  
255 *hiranonis BAI-17* to determine the nutrient utilization profile, and to to prepare an  
256 enhanced nutrient medium that can be used for large-scale culturing of this bacteria for  
257 screening, and preclinical and clinical studies. In addition, PM profiling of *P. hiranonis*  
258 *BAI-17* enabled comparison of the results to the published *C. difficile* PM profiles for  
259 shared metabolites of pathologic or therapeutic importance.<sup>36</sup>

260 The results indicate that 113 of 760 substrates in eight PM plates were utilized by  
261 *P. hiranonis BAI-17* (**Figure 6**). The most notable substrates that increased the growth of  
262 *P. hiranonis BAI-17* were glycyl-L-glutamic acid (64% increase in growth compared to  
263 negative control), pyroglutamic acid (54%), L-glutamine (52%), D, L,  $\alpha$ - amino-caprylic  
264 acid (49%), octopamine (49%), 2-aminoethanol (ethanolamine) (47%), p-hydroxy  
265 phenylacetic acid (p-HPA) (47%), and a group of dipeptides (up to 55% increase in  
266 growth). Based on the PM analysis, a selected subset of these substrates (glycyl-L-  
267 glutamic Acid, L-glutamine, 2-aminoethanol, 2-amino caprylic acid, and p-hydroxy  
268 phenylacetic acid) was included in culture media for further screening and propagation  
269 of *P. hiranonis*.

270 The observation that *P. hiranonis BAI-17* utilizes ethanolamine is significant. The  
271 ability to utilize ethanolamine has been shown to provide a nutritional growth advantage  
272 over other enteric bacteria since ethanolamine is abundant in mammalian gut epithelial  
273 cell membranes.<sup>37, 38</sup> Most importantly, ethanolamine catabolism has been demonstrated  
274 to induce the expression of virulence genes in *C. difficile*.<sup>37, 38</sup> Thus, the competitive  
275 ethanolamine utilization by *P. hiranonis BAI-17* may impact *C. difficile* virulence and  
276 growth in favorably from a bio-therapeutic perspective.<sup>36, 37</sup> Furthermore, the utilization  
277 of p-HPA by *P. hiranonis BAI-17* is notable in terms of *C. difficile* pathogenesis. p-HPA  
278 utilization is an important step in *C. difficile* tyrosine metabolism and induction of toxic  
279 p-cresol production, which has an important role in *C. difficile* overgrowth and CDI  
280 pathology in the gut.<sup>39-41</sup> Thus, competitive utilization of p-HPA by *P. hiranonis BAI-17*  
281 may significant impact *C. difficile* virulence in the gut. In short, PM method provides  
282 critical information to formulate an optimum growth medium for large-scale culturing of  
283 the candidate bacterium and to understand the therapeutically relevant competitive  
284 substrate utilization profile from an anti-*C. difficile* biotherapeutic perspective.

285 ***P. hiranonis BAI-17* exhibits robust bile acid deconjugation and 7- $\alpha$**   
286 **hydroxylation activities and inhibits *C. difficile* growth and toxin production**  
287 ***in vitro***

288 As described above, the genomic analysis of *P. hiranonis BAI-17* identified both  
289 *bai* and *bsh* genes and predicted both bile acid hydrolysing and 7- $\alpha$  hydroxylation ability.  
290 To confirm the functional *bai* and *bsh* expression of *P. hiranonis BAI-17* *in vitro*, a  
291 primary to secondary bile acid conversion (7- $\alpha$  dehydroxylation) and bile acid hydrolysis  
292 assays were performed separately. The results demonstrated that *P. hiranonis BAI-17*  
293 deconjugated taurocholic acid (TCA) (a predominant conjugated primary bile acid in gut)  
294 to cholic acid (CA) in BHIS medium within 48 h as evident by the complete  
295 disappearance of taurine conjugate and appearance of CA in the media (**Figure 7A**). This  
296 observation confirms the presence of a functional *bsh* gene in *P. hiranonis BAI-17*. Thus,  
297 *P. hiranonis BAI-17* need not depend on other gut commensals for initial bile acid  
298 hydrolysis of conjugated primary bile acids secreted from the liver.

299 Further, an *in vitro* bile acid conversion assay was performed to confirm the  
300 functionality of the *bai* operon in *P. hiranonis BAI-17*. As expected, our *P. hiranonis*  
301 isolate converted cholic acid to deoxycholic acid within 24 h in BHIS medium as evident  
302 by complete disappearance of CA and appearance of its secondary bile acid (deoxycholic  
303 acid-DCA) (**Figure 7B**). The molar difference between the products and substrates in  
304 both deconjugation and 7- $\alpha$  hydroxylation assays indicate the formation of intermediate  
305 metabolites.<sup>32, 42</sup> In summary, the *in vitro* bile acid assay together with comparative  
306 genomic analysis of available human and canine isolates establishes *P. hiranonis* as a bile  
307 acid deconjugating and 7- $\alpha$  hydroxylating bacterial species that has immense therapeutic  
308 potential.

309 Since the primary purpose of the screening pipeline is to identifying potential  
310 candidates for preclinical CDI infection trials, an *in vitro* *C. difficile* coculture experiment  
311 was included in the screening protocol. The *bai* operon-containing bacteria, *C. scindens*  
312 is a well-established candidate bacterium known to prevent *C. difficile* growth and  
313 virulence *in vitro* and *in vivo* in a bile acid-dependent manner.<sup>19, 43, 44</sup> Although less widely  
314 isolated in laboratories, it is known that *P. hiranonis* is associated with notable  
315 colonization resistance of *C. difficile* in dogs.<sup>25</sup> Since the bile acid metabolizing activity  
316 of *P. hiranonis* BAI-17 has already been established from the previous steps described  
317 above, we expected to find similar results with *P. hiranonis* *in vitro*. Indeed, the *in vitro*  
318 coculture experiment demonstrated that *P. hiranonis* BAI-17 inhibits *C. difficile* growth  
319 in the presence of micromolar concentrations of cholic acid (CA) in a dose-dependent  
320 manner (**Figure 7C**) (p<0.005). This could be attributed to production of the secondary  
321 bile acid (deoxycholic acid (DCA), in this assay) with or without the secretion of other  
322 antibacterial molecules inhibitory to *C. difficile* growth.<sup>44, 45</sup> A concomitant reduction *C.*  
323 *difficile* toxins (total toxin A and B) was also observed in a cholic acid-dependent manner  
324 (p<0.005). Interestingly, in the absence of cholic acid, the toxin production was either  
325 unchanged or increased despite the reduction in bacterial growth, underscoring the bile  
326 acid dependent anti-*C. difficile* properties of *P. hiranonis* BAI-17 (**Figure 7D**).

327 **ASF<sup>+</sup> mice experiment confirms *in vivo* bile acid conversion, potential non-host  
328 specific gut colonization ability and safety of *P. hiranonis* BAI-17**

329 For the final step of the screening pipeline, a mice experiment was designed to  
330 determine if the results obtained *in vitro* could also be observed *in vivo*. This experiment  
331 quantitatively confirms the ability of a bacterium to perform 7- $\alpha$  hydroxylation in the gut  
332 environment. Since, conventionally reared mice (Conv-R) harbor a complex microbiome,  
333 which may contain multiple bile acid metabolizing bacteria, testing a bacterium for *bai*

334 activity in relation to the gut bile acid profile is challenging. At the same time, using  
335 germ-free or gnotobiotic mice also has several limitations, including the lack of a  
336 functional 'host-gut microbiome interface', compromised immune system, diminished  
337 physiologic functions, and the need for costly animal care facilities. The interplay  
338 between the host-gut microbiome interface and the intestinal metabolites, specifically bile  
339 acids, is complex and requires a minimalistic but functional model for such studies.<sup>16, 24</sup>

340 The Altered Schaedler flora (ASF) is a murine bacterial consortium comprised of 8 known  
341 species<sup>46</sup>. Unlike germ-free or mono-associated animals with deficiencies in immune  
342 system development and function, mice colonized with the ASF possess a stable  
343 microbiome and normal immune and physiologic functions compared to Conv-R.<sup>46, 47</sup>

344 Moreover, ASF mice can be maintained in a non- gnotobiotic environment for several  
345 weeks, since the defined resident microflora is stable.<sup>46, 47</sup>

346 To establish the suitability of ASF mice for assaying bile acid metabolism *in vivo*,  
347 the annotated genomes of all eight ASF consortium members<sup>48</sup> are examined and  
348 confirmed that none of the ASF contains the *bai* operon. In contrast, four of the ASF  
349 members were predicted to encode *bsh* gene. These observations indicate that the ASF is  
350 a suitable model to quantify and assess 7- $\alpha$  dehydroxylation ability by heterologous  
351 microorganisms *in vivo*. Also, these experiments could also provide *in vivo* safety and  
352 toxicity assessment of the candidate bacterium, confirming the genome-wide virulence  
353 screening performed in the preceding steps of the screening pipeline. The same  
354 experiments could also provide insight into the inter-host colonizing ability (canine strain  
355 in this case) of the candidate bacterium that has significance in treating CDI in different  
356 mammalian species.

357 **P. hiranonis BAI-17 readily colonizes the ASF mouse gut**

358         Results showed that a single oral gavage of  $10^5$  CFU of *P. hiranonis* BAI-17 in  
359         adult ASF mice resulted in functional gut colonization of this bacterium. This observation  
360         is based on detection and visualization of *P. hiranonis* BAI-17 DNA and RNA in the gut  
361         3-weeks post-inoculation using qRT-PCR and RNAscope *in situ* hybridization methods,  
362         respectively. Positive amplification was observed in the colonic contents of all ASF mice  
363         inoculated with *P. hiranonis* BAI-17 (ASF-PH mice) euthanized at 9-weeks of age  
364         (**Figure 8D**), while no *P. hiranonis* BAI-17 specific amplification was observed in control  
365         ASF mice. In addition, RNAscope *in situ* hybridization of colonic tissue sections from  
366         mice euthanized 3- weeks post-inoculation revealed localization of *P. hiranonis* BAI-17  
367         in both luminal contents and within the tight mucus layer of the colonic mucosa (**Figure**  
368         **8A, B &C**). No positive signal was observed in control ASF mice.

369         **P. hiranonis BAI-17 colonization does not produce adverse effects in mice**

370         Clinical, gross, and histologic examination revealed no adverse enteropathologic  
371         changes in ASF mice colonized with *P. hiranonis*. Histopathology did not reveal  
372         significant inflammatory, toxic or degenerative changes in the gastrointestinal system of  
373         ASF and ASF-PH mice (data not shown).

374         **P. hiranonis colonization alters the gut bile acid profile**

375         As expected, the secondary bile acids DCA and LCA were not detected in ASF  
376         control mice, whereas a significant amount of these secondary bile acids was present in  
377         the colonic contents of ASF-PH mice (**Figure 9**). The DCA concentration in ASF-PH  
378         mice gut attained the same levels of CA indicating robust 7- $\alpha$  dihydroxylation activity of  
379         *P. hiranonis* BAI-17. This finding confirmed the *in vivo* bile acid converting ability of *P.*  
380         *hiranonis*. Most of the detected bile acids were unconjugated, indicating effective bile  
381         salt hydrolysis or ileal absorption of the remaining conjugated bile acids. Primary bile  
382         acids CDCA and  $\alpha$ -epimer of MCA were significantly elevated in ASF mice compared

383 to ASF-PH mice, presumably due to lack of 7- $\alpha$  dihydroxylation and conversion to  
384 secondary bile acids (p<0.05). Minimal CDCA with a high LCA concentrations in ASF-  
385 PH mice indicates a robust CDCA to LCA conversion. Thus, this study effectively  
386 demonstrated the *in vivo* bile acid conversion of our candidate bacterium. As detailed  
387 previously, the depletion of *bai*-containing bacteria (e.g., post-antibiotic treatment) is a  
388 major cause for bile-acid dysmetabolism and gut *C. difficile* overgrowth in susceptible  
389 individuals. Moreover, the ASF gut microbiota recapitulates a *bai*-depleted gut  
390 environment due to its limited microbiota composition. Thus, effective, non-pathogenic  
391 and functional colonization of *P. hiranonis* BAI-17 by filling this depleted *bai* niche in  
392 the ASF mice validates the therapeutic potential of this bacterium. Therefore, follow-up  
393 preclinical and clinical trials using *P. hiranonis* BAI-17 are likely to provide promising  
394 results as an effective anti-*C. difficile* biotherapeutic agent.

## 395 **Discussion**

396 Only a few species of 7- $\alpha$  dehydroxylating bacteria are known to be present in the  
397 mammalian gut. Almost all of them are members of the order Clostridiales and include  
398 *C. scindens*, *C. hylemonae*, *P. hiranonis*, some strains of *C. bif fermentans*, and *C. sordelli*,  
399 and a few species of *Lachnospiraceae* and *Ruminococcaceae* families. These bacteria  
400 contain the unique *bai* operon in their genome that consists of the *baiABCDEF* gene  
401 cluster, which performs sequential steps in the colonic conversion of primary bile acids  
402 to secondary bile acids in mammals, including humans.<sup>17</sup> Almost all the 7- $\alpha$   
403 dehydroxylating bacteria are fastidious slow-growing anaerobes with poorly known  
404 growth characteristics and virtually non-existent specific isolation and culture protocols.  
405 Among these bacteria, *C. scindens* is the only one that has been characterized to a greater  
406 extent and been used for current research on bile acid metabolism and CDI precision

407 microbiome therapy.<sup>20, 43, 49, 50</sup> Hence, identifying new culturable strains of *bai*-containing  
408 bacteria with robust bile acid converting ability is critical from a biomedical research and  
409 therapeutic perspective. For achieving this goal, the development of a more defined and  
410 utility-specific screening pipeline is required. Therefore, a pipeline was developed in this  
411 study that specifically screens *bai*-containing bacteria that have a defined anti-*C. difficile*  
412 therapeutic potential.

413 The screening pipeline detailed in this study is specifically intended for isolating  
414 live biotherapeutic bacterial candidates for precision microbiome-based CDI prophylaxis  
415 and treatment. To test this fecal screening pipeline, dogs were used as model donors, since  
416 they are inherently resistant to clinical CDI despite asymptomatic *C. difficile* carriage.<sup>25</sup>  
417 In addition, dogs are known to carry a high proportion of bile acid converting bacteria  
418 specifically *P. hiranonis* in their gut.<sup>51</sup> Moreover, *P. hiranonis* colonization is inversely  
419 associated with gut dysbiosis and *C. difficile* carriage, a parameter clinically used for  
420 assessing the gut dysbiosis index in dogs.<sup>25, 52, 53</sup> However, this pipeline described in this  
421 study has the flexibility to use any donor feces for isolating *P. hiranonis* and other *bai*-  
422 containing bacteria from any species.

423 Susceptible patients, especially the elderly, acquire CDI as a consequence of  
424 intensive antibiotic treatment, mainly beta-lactams and fluoroquinolones, administered  
425 for infections or surgical procedures. These antibiotics deplete the bile acid metabolizing  
426 bacterial flora in the gut, resulting in *C. difficile* gut colonization and overgrowth. In  
427 principle, CDI can be prevented by supplementing with robust bile acid metabolizing  
428 bacteria during administration of these antibiotics. Therefore, a *bai*-containing bacterium  
429 that can also withstand beta-lactam and fluoroquinolone pressure is a desirable target.  
430 Similarly, from a therapeutic viewpoint, a *bai*-containing bacterium with similar growth  
431 and nutrient requirements as *C. difficile* could have a competitive advantage when used

432 alone or as enrichment for FMT. Thus, a medium containing a beta-lactam antibiotic  
433 (moxalactam), a fluoroquinolone (norfloxacin), and a conjugated primary bile acid  
434 (taurocholate), along with other nutrients (e.g., cysteine and blood), were selected for  
435 screening the *bai* containing bacteria from fecal samples. This method effectively yielded  
436 five bile acid-converting bacterial isolates of three different species from 50 fecal samples  
437 tested (10%), including one (*P. hiranonis* BAI-17) that passed all the subsequent  
438 screening steps involved in this isolation pipeline, making it into the infection trial phase.  
439 In addition, a widely used medium for isolating *C. difficile* from fecal samples (CCFA  
440 medium supplemented with taurocholate) was also investigated for isolating *bai*-  
441 containing bacteria. The *C. difficile* yield from this method was higher compared to the  
442 TMNF medium; however, the isolation rate of *bai*-containing bacteria was very low, i.e.,  
443 4.77% with no *P. hiranonis* isolates (**supplementary table 1**). Another caveat with this  
444 method is that the CCFA medium does not contain a fluoroquinolone antibiotic, and  
445 hence the candidate bacterium may not be suitable for prophylactic use along with  
446 fluoroquinolones.

447 The next step involved in the screening process was to verify genes in the  
448 candidate bacterium and their functional activity associated with functional bile acid  
449 metabolism, virulence, and antibiotic resistance. Screening for specific genes associated  
450 with therapeutic significance of several candidate probiotic bacteria has been  
451 conventionally done using detections via PCR amplification.<sup>54</sup> However, our approach  
452 was to utilize next-generation sequencing, since it is now affordable and could provide  
453 comprehensive information on hundreds of genes and functional pathways  
454 simultaneously. Thus, we adopted WGS sequencing using the Illumina MiSeq platform  
455 for this purpose. Annotation of the assembled sequences confirmed the presence of *bai*  
456 genes in *P. hiranonis* BAI-17. However, identifying a *bsh* gene at this step further

457 demonstrated the therapeutic value of the *P. hiranonis* BAI-17 isolate. Generally, bile acid  
458 deconjugation in the gut is carried out by a set of bacteria that are primarily members of  
459 the phyla Bacteroidetes and Firmicutes. Notable bile salt hydrolysers in the gut include  
460 several species of *Bacteroides*, *Parabacteroides*, *Listeria*, *Bifidobacterium*, and  
461 *Lactobacillus*.<sup>17</sup> Presence of a functional *bsh* has not been demonstrated yet in any other  
462 *bai* containing bacterial species. A few clostridial species, such as *C. perfringens* and *C.*  
463 *botulinum* contain *bsh* genes; however, they do not possess the *bai* operon.<sup>31, 55</sup> The *bai*  
464 operon of *P. hiranonis* is comparable to that of other widely known bile acid converting  
465 bacteria namely *C. scindens* and *C. hylemonae*, which does not contain the *bsh* gene.<sup>56</sup>  
466 The complete genome assembly of *P. hiranonis* BAI-17 and comparative genome analysis  
467 data suggest a close genetic relationship between *P. hiranonis* (both canine and human  
468 isolates) and the well-known *bai*-containing bacteria *C. hylemonae*, and *C. scindens*  
469 although neither of them contains *bsh*. The functional activity of both *bsh* and *bai* of *P.*  
470 *hiranonis* is confirmed by the *in vitro* bile acid conversion tests, which includes a bile salt  
471 conjugation assay (for *bsh* activity) using the conjugated primary bile acid TCA and 7- $\alpha$   
472 dehydroxylation assay (for *bai* activity) with the primary bile acid, CA. Further, the  
473 animal experiment (ASF<sup>+</sup> mouse test) confirmed *in vivo* formation of secondary bile acid  
474 in *P. hiranonis* colonized mice suggesting that this bacterium could exert a therapeutic  
475 effect in the gut environment. Therefore, the novel ASF<sup>+</sup> mouse model for specifically  
476 and quantitatively assessing bacterial 7- $\alpha$  dehydroxylation has been shown to be effective  
477 in meeting this purpose.

478 The WGS step included in the screening pipeline also provides a comprehensive  
479 picture of potential and putative virulence factors in the candidate bacterium. Members  
480 of the family Clostridiaceae, to which *P. hiranonis* belongs, are known for different  
481 exotoxins, including pore-forming toxins, phospholipase C, collagenase, large

482 glucosylating toxins, binary toxins, and neurotoxins.<sup>57</sup> The annotation of *P. hiranonis*  
483 *BAI-17* sequence assembly did not identify any known toxins or superantigens in its  
484 genome, which predicted the safety of this bacterium for therapeutic use. This observation  
485 was further confirmed *in vivo* by the absence of tissue lesions and adverse signs in ASF-  
486 PH mice post-inoculation. In addition, WGS sequencing also confirmed fluoroquinolone  
487 and beta-lactam resistance in the candidate bacterium, which corroborates with the  
488 selection pressure and screening process using the TMNF media. Since *C. difficile* is  
489 inherently resistant to these antibiotics, horizontal transfer of the resistance genes from  
490 the candidate bacterium to the pathogen is not a concern in this case.

491 WGS results also identified fibronectin-binding proteins (FBPs) in the *P.*  
492 *hiranonis* *BAI-17* genome. Fibronectin is widely expressed in the intestinal epithelium of  
493 mammals and is widely utilized by gut bacteria for mucosal adhesion.<sup>58, 59</sup> FBPs in  
494 bacteria, including probiotic species such as *L. plantarum* and pathogens such as *C.*  
495 *difficile*, are involved in gut colonization and long-term retention of the bacterium in the  
496 intestinal lumen.<sup>54, 58, 60-62</sup> Moreover, detection of FBP gene within the bacterial genome  
497 has been utilized to predict putative intestinal colonization of probiotic bacteria.<sup>54</sup> Thus,  
498 although speculative, having this gene expressed could help *P. hiranonis* *BAI-17* to  
499 colonize the recipient animals independent of the host species. Interestingly, the *in vivo*  
500 experiment in this study demonstrated that a single oral dose of *P. hiranonis* *BAI-17*  
501 resulted in stable functional gut colonization of this bacterium in the adult ASF mice gut,  
502 which was confirmed by detection of this bacterium in the feces and production of  
503 secondary bile acids three weeks post-inoculation. This finding indicates the colonization  
504 potential of *P. hiranonis* *BAI-17* in a functionally and structurally dysbiotic gut (found  
505 ASF mice) of other non-hosts species including humans, horses and swine with CDI.  
506 Moreover, fibronectin binding using Fbp68 is crucial for *C. difficile* gut colonization.<sup>61</sup>

507 63-65 Phylogenetic analysis of *P. hiranonis* FBP (including canine *P. hiranonis* BAI-17  
508 and DGF055142, and human DSM13275) using BLASTn revealed that the closest  
509 bacterial gene predicted was the FBP of *Romboutsia* sp (query cover 99%, E value: 0, and  
510 percentage identity 71%) and *C. difficile* (query cover 99%, E value: 0, and percentage  
511 identity 69%). Thus, it is also likely that *P. hiranonis* BAI-17 would inhibit *C. difficile*  
512 colonization by competitive exclusion, adding to the therapeutic potential of this  
513 bacterium, and a question of interest in future studies.

514 Additionally, Biolog PM provided a set of metabolites that when supplemented in  
515 media enhances the *in vitro* growth of *P. hiranonis* BAI-17. This information enabled the  
516 formulation of an enhanced growth media for this bacterium. Although not tested in this  
517 study, it is also likely that the TMNF medium supplemented with these metabolites will  
518 allow an increased isolation rate of *P. hiranonis* strains. In addition, as detailed in results,  
519 utilization of ethanolamine, which is associated with virulent strains of *C. difficile*, could  
520 add to the biotherapeutic potential of *P. hiranonis* BAI-17 as it may compete with *C.*  
521 *difficile* for this metabolite.<sup>37, 38</sup> Phenotypic microarrays also indicated the utilization of  
522 pHPA by *P. hiranonis* BAI-17. pHPA is important in *C. difficile* pathogenesis as this  
523 pathogen converts pHPA to p-cresol. This toxic compound inhibits the growth of other  
524 bacteria in the gut and contributes to dysbiosis and *C. difficile* overgrowth.<sup>66, 67</sup> *C. difficile*  
525 contains the *hpdBCA* operon involved in production of p-cresol from its precursor  
526 molecule pHPA.<sup>39</sup> Interestingly, the WGS data revealed an absence of the *hpd* genes in  
527 *P. hiranonis* BAI-17, suggesting that pHPA utilization by this bacterium is not associated  
528 with p-cresol production. Thus, competitive utilization of pHPA by *P. hiranonis* BAI-17  
529 may result in fewer precursors available for p-cresol production, which will also  
530 contribute to its therapeutic significance.

531 In summary, the isolation pipeline, which involve fecal screening in TMNF  
532 media, WGS analysis, phenotype microarrays, *in vitro* bile conversion analysis, and *C.*  
533 *difficile* inhibition assays, as well as proof of concept *in vivo* studies (ASF<sup>+</sup> mouse test)  
534 has been described. This protocol has been shown to efficiently isolate *bai*-containing  
535 bacteria from fecal samples, identify broad CDI-specific therapeutic characteristics, and  
536 determine the pathogenicity and safety. Thus, a bacterium that met all the criteria set can  
537 be passed to more extensive preclinical infection trials. In addition, the salient  
538 confirmation that *P. hiranonis* harbors both *bai* and *bsh* genes essential for bile acid  
539 conversion makes this bacterium therapeutically appealing. Altogether, the screening  
540 pipeline developed for bile acid converting bacteria revealed the unique anti-*C. difficile*  
541 biotherapeutic potential of *P. hiranonis* and these findings can be validated by follow-up  
542 infection studies in mice and subsequent clinical trials.

543 **Materials and methods**

544 **Overview of the screening pipeline for *bai*-containing bacteria**

545 The screening pipeline for isolating *bai*-containing bacteria with anti-*C. difficile*  
546 therapeutic potential has the following objectives: a) isolation of a *bai*-containing  
547 bacterium that can grow along with *C. difficile* and has similar competitive growth  
548 requirements and identical resistance pattern to bile acids, antibiotics and other gut derived  
549 chemicals as exhibited by *C. difficile*; b) genotypic screening of the candidate bacteria for  
550 virulence factors and other genetic attributes that has putative therapeutic advantage  
551 against *C. difficile*; c) phenotypic screening for metabolites that influence the growth of  
552 the candidate bacteria for identifying specific growth medium and future species specific  
553 screening medium; d) *in vitro* screening of the candidate bacteria for bile acid  
554 transformation activity and bile-acid dependant *C. difficile* inhibitory effect; e) *in vivo*  
555 screening for quantitative bile acid conversion ability in the gut environment in a *bai*-

556 depleted animal model (ASF mice) which enables parallel assessment of gut colonization  
557 ability and potential tissue-organ toxicity. The overview of this pipeline and steps  
558 involved for meeting these objectives are depicted in **Figure 1**.

559 **Donor animals, sampling, and isolation of *bai*-containing bacteria from canine**  
560 **fecal samples**

561 Random canine fecal samples were collected from multiple sources at Iowa State  
562 University (ISU) College of Veterinary Medicine: 1) small animal teaching hospital,  
563 Lloyd Veterinary Medical Center, 2) Department of Veterinary Pathology, and 3) ISU  
564 Veterinary Diagnostic Laboratory (VDL). Fifty random samples were used for screening  
565 in TMNF medium (modified *C. difficile* Moxalactam Norfloxacin medium with 0.1%  
566 taurocholate), and 250 samples were used for screening in CCFA medium as  
567 previously.<sup>27, 30</sup> Approximately 1g of feces was resuspended in 10 mL of pre-reduced  
568 TMNF broth, mixed thoroughly and incubated in an anaerobic workstation (AS-580,  
569 Anaerobe Systems, Morgan Hill, CA, USA) for 7 days in anaerobic condition (0%  
570 oxygen, 5% hydrogen, 5% CO<sub>2</sub> and 90% nitrogen at 37°C). After enrichment, the  
571 suspension was then centrifuged at 5000 rpm for 15 minutes. The supernatant was  
572 removed, the pellet was transferred to the anaerobic workstation, resuspended in 0.2 mL  
573 of TMNF broth, mixed thoroughly, and immediately plated onto pre-reduced nonselective  
574 blood agar (R01202, Fisher Scientific, Waltham, MA) and BHIS agar (Brain Heart  
575 Infusion supplemented with 0.5% yeast extract), and incubated at 37°C for 48 h in  
576 anaerobic condition as described above. After visible growth, colonies were tested for an  
577 L-proline aminopeptidase activity with PRO Disk (ThermoFisher Scientific, Waltham,  
578 MA, USA), to screen for *C. difficile* and bile acid converting bacteria *C. sordellii*, *C.*  
579 *bif fermentans*, and *P. hiranonis*<sup>29</sup>) per the manufacturer's instructions. Test positive  
580 colonies were subcultured onto CDMN agar and incubated for 24-48 h to obtain pure

581 culture of each colony. After 48 h, the pure growths were harvested and subcultured in  
582 BHI broth for further experiments

583 **Bacterial identification**

584 The identity of the candidate bacterium was determined using matrix-assisted  
585 laser desorption–ionization time-of-flight mass spectrometry (MALDI-TOF) and further  
586 confirmed by 16s rRNA PCR sequencing. The sample preparation and analysis were  
587 carried out as previously described.<sup>68</sup> For PCR and sequencing, the broth culture was  
588 centrifuged at 5,000 x g at 4°C for 15 minutes. The supernatant was discarded, and the  
589 DNA was extracted from the bacterial pellet using the QIAamp BiOstic Bacteremia DNA  
590 Kit (Qiagen, Germantown, MD, USA). Extracted DNA was amplified by traditional PCR  
591 using universal 16S rRNA gene targeting primers. PCR was performed using Promega  
592 GoTaq® Master Mixes with the following thermocycler conditions: initial denaturation  
593 at 95°C for 3 minutes followed by 30 cycles of denaturation at 95°C for 30 seconds,  
594 annealing at 55°C for 30 seconds and extension at 65°C for 45 seconds and a final  
595 extension at 72°C for 3 minutes. Amplification was confirmed with gel electrophoresis  
596 using a 1% agarose gel. DNA sequencing was performed at the ISU DNA Facility with  
597 an automated DNA sequencer (ABI 3130XL; Applied Biosystems Instrument, Carlsbad,  
598 CA, USA). The results blasted with NCBI GenBank database for species assignment.

599 **Whole-genome sequencing**

600 Two separate genomic DNA libraries were prepared according to the  
601 requirements of the Illumina and Oxford Nanopore systems. A combination of long-read  
602 Nanopore MinION and short-read Illumina MiSeq platforms was used to generate the  
603 complete genome sequence of the *P. hiranonis* BAI-17 strain. For Illumina sequencing,  
604 the extracted genomic DNA was fragmented by sonication using a Covaris M220

605 sonicator (Covaris, Woburn, MA, USA). The trimmed DNA fragment sequences were  
606 then used to prepare a shotgun paired-end library with an average insert size of 350 bp  
607 using a TruSeq DNA Sample Prep kit (Illumina, San Diego, CA, USA). The library was  
608 sequenced on an Illumina MiSeq platform (Illumina, San Diego, CA, USA) using the  
609 150-bp paired-end sequencing mode. Base calling of the two paired FASTQ files were  
610 done with the Illumina raw sequence read data. The quality of the raw sequence reads  
611 was assessed using FastQC v0.11.8, and Trimmomatic v0.39 was used to trim sequencing  
612 adapter reads with a quality score <20 at 3' and 5' ends.<sup>69</sup> After trimming the adaptors and  
613 filtering low-quality reads, the clean sequence data were used for further bioinformatics  
614 analyses. For Nanopore sequencing, a MinION sequencing library was prepared using  
615 the Nanopore Ligation Sequencing Kit (SQK-LSK109; Oxford Nanopore, Oxford, UK).  
616 The library was sequenced with an R9.4.1 MinION flow cell (FLO-MIN106) for a 24 h  
617 run using MinKNOW v2.0 with the default settings. FAST5 files containing raw  
618 Nanopore signal data were base-called and converted to FASTQ format in real-time using  
619 Guppy v3.3.0, after which Porechop v0.2.4 was used to trim barcode and adapter  
620 sequences. Filtlong v0.2.0, a quality filtering tool for Nanopore reads, was used to remove  
621 sequences shorter than 3000 bases and with mean quality scores of less than 12 to  
622 facilitate assembly.

623 ***De novo genome assembly and comparative phylogenomic analysis***

624 Hybrid de novo genome assembly was performed using Unicycler v0.4.8, which  
625 allows for both Illumina reads (short, accurate) and Nanopore reads (long, less accurate)  
626 to be used in the conservative mode.<sup>70</sup> The highly accurate Illumina reads were aligned  
627 against the Nanopore reads as a reference to correct random sequencing errors and finally  
628 create a genome assembly of high quality. Ultimately, the assembled sequence was  
629 polished by aligning the Illumina paired-end reads with the BWA-MEM algorithm using

630 Pilon v1.2.3 for several rounds to improve genome assembly quality.<sup>71</sup> Multiple rounds  
631 of error correction were performed until no more errors could be fixed. The quality of the  
632 assembled genome was assessed using Quast.<sup>72</sup> Finally, the complete genome sequence  
633 of *P. hiranonis* BAI-17 strain was annotated using Prokka 1.14.6.<sup>73</sup>

634 The *P. hiranonis* BAI-17 strain was phylogenomically compared with other  
635 known primary bile acid converting species. To this end, seven genomes of *Clostridium*  
636 *scindens* (*Clostridium scindens* BL389WT3D, *Clostridium scindens* VE202-05,  
637 *Clostridium scindens* MSK.1.26, *Clostridium scindens* BL-398-WT-3D, *Clostridium*  
638 *scindens* MGYG-HGUT-01303, *Clostridium scindens* MSK.1.16, *Clostridium scindens*  
639 ATCC35704), four genomes of *Clostridium hylemonae* (*Clostridium hylemonae* MGYG-  
640 HGUT-01710, *Clostridium hylemonae* DSM15053, *Clostridium hylemonae* DSM-15053,  
641 *Clostridium hylemonae* BSD2780061688st1\_A6, *Clostridium hylemonae*  
642 BSD2780061688b-171218\_A6) and one human origin *P. hiranonis* genome (*P. hiranonis*  
643 DSM 13275) were downloaded from the National Center for Biotechnology Information  
644 (NCBI) and compared against the genome of *P. hiranonis* BAI-17 strain using Anvio  
645 version 6.2.<sup>74</sup> Briefly, first, an 'Anvi'o genomes storage database' was generated from the  
646 FASTA files of 14 isolate genomes from *P. hiranonis* BAI-17, *C. scindens*, and *C.*  
647 *hylemonae* using the '--external-genomes' flag and Anvi-pan-genome' with the genomes  
648 storage database, the flag '--use-NCBI-blast,' parameters '--minbit 0.5', and '--mcl-  
649 inflation 10' were then employed to calculate similarities of each amino acid within each  
650 genome, and remove weak, originally described in ITEP, to filters out weak hits based on  
651 the aligned fraction between two reads.<sup>75 76</sup> The MCL algorithm identified gene clusters  
652 in the remaining Blastp search results. Hence, it computed the occurrence of gene clusters  
653 across genomes and the total number of genes they contain. This generated a hierarchical  
654 clustering analysis for gene clusters (based on their distribution across genomes) and

655 genomes (based on gene clusters they share) using a default Euclidean distance and Ward  
656 clustering. The final product was a generated anvi'o pan database that stored all results  
657 for downstream analyses to be visualized by the 'anvi-display-pan program.<sup>77</sup>' Anvi'o  
658 also contains anvi-compute-genome-similarity, a program that uses various similarity  
659 metrics, such as PyANI, to compute average nucleotide identity (ANI) across genomes,  
660 and Sourdough to compute mash distance across genomes. The GFF3 file containing both  
661 sequences and annotations was used to compare and identify candidate genes based on  
662 Venn diagrams.<sup>78</sup>

### 663 **Phenotype microarrays**

664 The *P. hiranonis* BAI-17 strain was grown overnight in a pre-reduced BHI broth  
665 medium supplemented with 0.3% sodium taurocholate inside the anaerobic chamber (Coy  
666 Laboratories, Grass Lake, MI, USA). Approximately 200 µl of the overnight culture was  
667 anaerobically plated on prereduced BHI agar supplemented with 0.3% sodium  
668 taurocholate. The agar plates were anaerobically incubated at 37°C for 72 h (to ensure a  
669 thick layer of growth of bacteria). Then, sterile cotton swabs were used to pick the  
670 bacterial culture from the plate without reaching the agar plate surface and mixed with  
671 the anaerobic BIOLOG buffer. A baseline OD630 value of ~0.02 for the buffer was  
672 ensured before substrate OD measurement. One hundred microliters of the OD630 ~0.02  
673 buffer was pipetted into each well of the BIOLOG PM1-PM8 plates in quadruplets. The  
674 OD630 for the bacterial and buffer mixture was measured using a flat bottom untreated  
675 96 well plate with the Bio-tek Microplate reader (Elx808). OD630 readings were taken at  
676 0 h and 24 h. Final OD values were divided by initial OD values to obtain fold changes  
677 in growth. The mean of the four replicates was calculated and normalized by mean fold  
678 change in the negative control to calculate % bacterial growth in each substrate. Twenty

679 percent or greater growth in the substrate, when compared to control, was considered as  
680 significant growth.

681 **Bile acid transformation assays**

682 All bile acid-containing media and controls (without bile acid) were inoculated  
683 with 200  $\mu$ L of 18 h old *P. hiranonis* BAI-17 strain culture. Freshly prepared stock  
684 solutions of all bile acids (CA, CDCA and TCA) were prepared using solvents (ethanol  
685 for CA and CDCA and water for TCA) and subsequently added to 20 mL BHI broth to  
686 reach a final concentration of 50  $\mu$ M for the respective bile acid. The tubes were incubated  
687 in the anaerobic workstation (AS-580, Anaerobe Systems, Morgan Hill, CA, USA) at  
688 37°C for 72 h. A sterile control and an additional control without bile acid (but with the  
689 ethanol vehicle) were included in triplicates for this experiment. Culture samples were  
690 drawn at 0h, 12h, 24h, 48h, and 72h, and the OD600 was measured soon afterward. Each  
691 sample (1 ml) was centrifuged at 5,000  $\times$  g at 4°C for 15 minutes. The supernatant was  
692 collected and aliquoted to multiple microcentrifuge tubes. All samples were stored at  
693 -20°C until bile acid analysis (described later in this section).

694 **Coculture experiments, bacterial growth and toxin quantitation**

695 Mono and Co-culture of *C. difficile* UK1 strain and *P. hiranonis* BAI-17 strain  
696 were done in BHIS medium (Brain Heart Infusion supplemented with 5 g/L yeast extract)  
697 with three concentrations of CA (0, 50, and 150  $\mu$ M).<sup>79, 80</sup> Cocultures, and the  
698 corresponding monocultures, were incubated in triplicate under anaerobic conditions at  
699 37°C for 48 h. Samples were drawn at 0 h, 24 h, and 48 h for the bacterial growth  
700 assessment by dilution and plating on pre-reduced blood agar and total toxin quantitation  
701 by ELISA. Each sample (1 mL) of each monoculture and coculture was centrifuged at  
702 5,000  $\times$  g for 15 min, and pellets and supernatants were collected and stored at -20°C.

703                   The supernatant was diluted and was assayed for *C. difficile* toxin A/B ELISA  
704                   using Techlab Tox A/B kit (Techlab, Blacksburg, VA, USA) per the manufacturer's  
705                   instructions. Quantification of the *C. difficile* total toxins A and B was based on the  
706                   standard curve of purified toxins generated previously.<sup>81</sup> The optical density was  
707                   measured at 450 nm and compared to the standard curve's linear range to determine total  
708                   toxin concentration.

709                   **Animals, inoculum preparation, and ASF+ mouse test**

710                   All animal experiments were performed in accordance with the protocols  
711                   approved by ISU Institutional Animal Care and Use Committee (IACUC-19-166,  
712                   IACUC-20-091). ASF mice were obtained from the in-house breeding colonies  
713                   maintained at the Vaccine Research Institute at ISU by Dr. Michael Wannemuehler. The  
714                   treatment groups were housed separately and provided with irradiated feed and  
715                   autoclaved water *ad libitum*. The integrity and composition of the ASF flora in the gut of  
716                   the mice were confirmed by routine fecal sampling, multiplex PCR for constituent ASF  
717                   flora, and 16S rRNA gene sequencing.<sup>46</sup> Nine, 6-week-old (young adult) ASF mice were  
718                   administered a single oral gavage dose of 100  $\mu$ l of  $1 \times 10^8$  CFU/mL *P. hiranonis* BAI-17  
719                   grown anaerobically in BHI medium for 24 h. Six ASF mice were kept as a control for  
720                   the study. For detection of *P. hiranonis* BAI-17 colonization, fresh fecal pellets were  
721                   collected from individual mice at 3 and 6-weeks post-inoculation. The animals were  
722                   euthanized at 3- and 6-weeks post-inoculation, and the cecal contents and intestinal tissue  
723                   samples were collected for further processing.

724                   **Real-time PCR**

725                   The fecal pellets from ASF mice were thawed, and the DNA was extracted using  
726                   the QIAamp PowerFecal proDNA kit (Qiagen, Germantown, MD, USA). DNA from *C.*

727 *butyricum*, a negative control, and *P. hiranonis* *BAI-17* positive control, were also  
728 extracted from pure cultures using the QIAamp BiOstic Bacteremia DNA kit (Qiagen,  
729 USA) according to the manufacturer's instructions. Custom canine *P. hiranonis* specific  
730 primers and probes were designed based on the whole genome sequence information of  
731 the *P. hiranonis* *BAI-17*, which consists of Forward:  
732 5'AAATAGGTGCTCAGAACATGCA3', Reverse:  
733 5'TCATCAGTTCGTTGAAGTACTGT3', and Probe: FAM-  
734 5'TGGAGCTTCACTGGAGAAGTTGCACCA3'-TAMRA. A TaqMan-based real-  
735 time PCR was then performed on the DNA samples using the QuantStudio 3 Real-Time  
736 PCR Systems (ThermoFisher Scientific, Waltham, MA, USA), using optical grade 96-  
737 well plates. Twenty microliter reactions were made using TaqPath™ 1-Step RT-qPCR  
738 Master Mix (ThermoFisher Scientific, Waltham, MA, USA), with 10  $\mu$ mol 1:1:1 ratio of  
739 forward/reverse primer, and probe and 20ng of DNA template for each reaction. The  
740 thermocycler conditions for real-time PCR were 95°C for 2 min, 95°C for 3 seconds for  
741 40 cycles, and 60°C for 30 seconds. Each sample was run in triplicate, and the mean  
742 values were calculated. In addition, an amplification plot was generated with the threshold  
743 cycle (CT) values, and automatic analysis settings determined baseline settings.

#### 744 **RNAscope® *in situ* hybridization and histopathology**

745 Gut colonization of *P. hiranonis* *BAI-17* in ASF mice (ASF<sup>+</sup>) was confirmed by  
746 RNA *in situ* hybridization using RNAscope®, described previously.<sup>82</sup> Briefly, custom  
747 paired B-*P. hiranonis*-16S (cat. 1057061-C1) double-Z oligonucleotide probes were  
748 designed against target RNA (16s rRNA) and probed region (ZZ probe targeting 17445  
749 to 17482 nt), using custom software. The RNAscope® 2.5 HD Red Reagent (Advanced  
750 Cell Diagnostics, Newark, CA) was used according to the manufacturer's instructions.  
751 Formalin-fixed paraffin-embedded (FFPE) tissue sections of 5  $\mu$ m thickness were

752 prepared according to the manufacturer's recommendations. Each sample was quality  
753 controlled for RNA integrity with a probe specific to the housekeeping gene. To achieve  
754 interpretable results, assays using archived FFPE tissues were run parallel with positive  
755 and negative controls. Negative control background staining was evaluated using a probe  
756 specific to the bacterial *dapB* gene. Brightfield/Fluorescent images were acquired using  
757 an Olympus Bx53 microscope (Olympus Optical Company, Tokyo, Japan) under 40x  
758 objective.

759 The colon and cecum were sectioned at 5 $\mu$ m thickness and stained with  
760 hematoxylin and eosin. Images of these sections were acquired with 100 $\times$  magnification  
761 using an Olympus BX53 microscope (Olympus Optical Company, Tokyo, Japan). The  
762 sections were evaluated by a board-certified pathologist.

### 763 **Targeted metabolomic analysis**

764 The targeted metabolomics analysis of fecal bile acids was performed by  
765 PennChop Microbiome and Metabolomics Core (Philadelphia, PA, USA) as described  
766 previously.<sup>83</sup> A Waters Acquity uPLC System with a QDa single quadrupole mass  
767 detector was used to measure bile acids. Fecal samples were suspended in methanol  
768 (5  $\mu$ L/mg stool), vortexed for 1 minute, then centrifuged twice for 5 minutes at 13,000  $\times$   
769 g. On an Acquity uPLC with a CorteCS UPLC C-18 + 1.6 mm 2.1 $\times$  50 mm column, the  
770 supernatants were examined. The flow rate was 0.8 mL/min, and the injection volume  
771 was 4  $\mu$ L, the column temperature was 30 °C, the sample temperature was 4 °C, with a  
772 run time of 4 minutes per sample. Eluent A was 0.1% formic acid in water; eluent B was  
773 0.1% formic acid in acetonitrile; the weak needle wash was 0.1% formic acid in water;  
774 the strong needle wash was 0.1% formic acid in acetonitrile. The seal wash was 10%  
775 acetonitrile in water. The gradient was 70% eluent A for 2.5 min, 100% eluent B for  
776 0.6 min, and then 70% eluent A for 0.9 min. The mass detection channels were: +357.35

777 for chenodeoxycholic acid and deoxycholic acid; +359.25 for lithocholic acid; -407.5 for  
778 cholic, alphanuricholic, betanuricholic, gamma muricholic, and omegamuricholic acids;  
779 -432.5 for glycolithocholic acid; -448.5 for glycochenodeoxycholic and  
780 glycideoxycholic acids; -464.5 for glycocholic acid; -482.5 for tarolithocholic acid;  
781 -498.5 for taurochenodeoxycholic and taurodeoxycholic acids; and -514.4 for  
782 taurocholic acid. Samples were quantified against standard curves of at least a five points  
783 run, performed in triplicate. Standard curves were done at the beginning and end of each  
784 metabolomics run. Quality control checks (blanks and standards) were run every eight  
785 samples. Results were rejected if the standards deviated by greater than  $\pm 5\%$ .

## 786 **Statistics**

787 Statistical analysis was performed using GraphPad Prism 9 (GraphPad Software,  
788 San Diego, CA). The results of the animal study were expressed as means  $\pm$  standard  
789 errors of the means (SEM). The differences between the experimental groups were  
790 compared using the analysis of variance (ANOVA). The differences between the two  
791 groups were analyzed using an unpaired Student's t-test. The statistical significance level  
792 was set at  $p < 0.05$ .

## 793 **Disclosure statement**

794 The authors declare no competing interest.

795

## 796 **Availability of data**

797 The genome data will be available at GenBank (<https://www.ncbi.nlm.nih.gov/genbank/>)  
798 following a 12-month embargo from the date of publication to allow for

799 commercialization of research findings. The data supporting the findings of this study are

800 available from the corresponding author SM on request after the embargo period.

801

802 **References**

803

- 804 1. Hookman P, Barkin JS. Clostridium difficile associated infection, diarrhea and  
805 colitis. *World JGastroenterol* 2009; 15:1554.
- 806 2. Songer JG, Uzal FA. Clostridial enteric infections in pigs. *JVetDiagnInvest* 2005;  
807 17:528.
- 808 3. Keel MK, Songer JG. The comparative pathology of Clostridium difficile-  
809 associated disease. *VetPathol* 2006; 43:225.
- 810 4. Britton RA, Young VB. Role of the intestinal microbiota in resistance to  
811 colonization by Clostridium difficile. *Gastroenterology* 2014; 146:1547.
- 812 5. Lessa FC, Mu Y, Bamberg WM, Beldavs ZG, Dumyati GK, Dunn JR, et al.  
813 Burden of Clostridium difficile Infection in the United States. *N Engl J Med* 2015;  
814 372:825.
- 815 6. @CDCgov. What is C. diff? | CDC. @CDCgov, 2021.
- 816 7. Songer JG. The emergence of Clostridium difficile as a pathogen of food animals.  
817 *Animal Health Research Reviews* 2004; 5:321.
- 818 8. Hensgens MP, Keessen EC, Squire MM, Riley TV, Koene MG, de Boer E, et al.  
819 Clostridium difficile infection in the community: a zoonotic disease? *ClinMicrobiolInfect*  
820 2012; 18:635.
- 821 9. Postma N, Kiers D, Pickkers P. The challenge of Clostridium difficile infection:  
822 Overview of clinical manifestations, diagnostic tools and therapeutic options.  
823 *IntJAntimicrobAgents* 2015.
- 824 10. Antibiotic Resistance Threats in the United States- 2013. Atlanta, GA: Centers for  
825 Disease Control and Prevention, 2013.
- 826 11. Weingarden AR, Dosa PI, DeWinter E, Steer CJ, Shaughnessy MK, Johnson JR,  
827 et al. Changes in Colonic Bile Acid Composition following Fecal Microbiota  
828 Transplantation Are Sufficient to Control Clostridium difficile Germination and Growth.  
829 *PLoS One* 2016; 11:e0147210.
- 830 12. Weingarden AR, Chen C, Bobr A, Yao D, Lu Y, Nelson VM, et al. Microbiota  
831 transplantation restores normal fecal bile acid composition in recurrent Clostridium  
832 difficile infection. *AmJPhysiolGastrointestLiver Physiol* 2014; 306:G310.
- 833 13. Monaghan T, Mullish BH, Patterson J, Wong GK, Marchesi JR, Xu H, et al.  
834 Effective fecal microbiota transplantation for recurrent Clostridioides difficile infection  
835 in humans is associated with increased signalling in the bile acid-farnesoid X receptor-  
836 fibroblast growth factor pathway. *Gut Microbes* 2019; 10:142-8.
- 837 14. Zellmer C, Sater MRA, Huntley MH, Osman M, Olesen SW, Ramakrishna B.  
838 Shiga Toxin-Producing *Escherichia coli* Transmission via Fecal Microbiota Transplant.  
839 *Clin Infect Dis* 2021; 72:e876-e80.
- 840 15. Glover SC, Burstiner S, Jones D, Teymoorian A, Naga Y, Silver J, et al. 2099 E.  
841 *coli* Sepsis Following FMT in an IgA Deficient IBD Subject. Official journal of the  
842 American College of Gastroenterology | ACG 2019; 114:S1170.
- 843 16. Jia W, Xie GX, Jia WP. Bile acid-microbiota crosstalk in gastrointestinal  
844 inflammation and carcinogenesis. *Nat Rev Gastro Hepat* 2018; 15:111-28.
- 845 17. Ridlon JM, Kang DJ, Hylemon PB. Bile salt biotransformations by human  
846 intestinal bacteria. *J Lipid Res* 2006; 47:241-59.
- 847 18. Li JN, Dawson PA. Animal models to study bile acid metabolism. *Bba-Mol Basis  
848 Dis* 2019; 1865:895-911.

- 849 19. Buffie CG, Bucci V, Stein RR, McKenney PT, Ling L, Gobourne A, et al.  
850 Precision microbiome reconstitution restores bile acid mediated resistance to *Clostridium*  
851 *difficile*. *Nature* 2015; 517:205-8.
- 852 20. Greathouse KL, Harris CC, Bultman SJ. Dysfunctional families: *Clostridium*  
853 *scindens* and secondary bile acids inhibit the growth of *Clostridium difficile*. *Cell Metab*  
854 2015; 21:9-10.
- 855 21. Sorg J, Sonenshein A. Bile salts and glycine as cogerminants for *Clostridium*  
856 *difficile* spores. *JBacteriol*, 2008:2505.
- 857 22. Tam J, Icho S, Utama E, Orrell KE, Gomez-Biagi RF, Theriot CM, et al. Intestinal  
858 bile acids directly modulate the structure and function of *C. difficile* TcdB toxin. *Proc*  
859 *Natl Acad Sci U S A* 2020; 117:6792-800.
- 860 23. Darkoh C, Brown EL, Kaplan HB, Dupont HL. Bile salt inhibition of host cell  
861 damage by *Clostridium difficile* toxins. *PLoS One* 2013; 8:e79631.
- 862 24. Abt MC, McKenney PT, Pamer EG. *Clostridium difficile* colitis: pathogenesis  
863 and host defence. *Nature Reviews Microbiology* 2016; 14:609-20.
- 864 25. Stone NE, Nunnally AE, Jimenez V, Jr., Cope EK, Sahl JW, Sheridan K, et al.  
865 Domestic canines do not display evidence of gut microbial dysbiosis in the presence of  
866 *Clostridioides* (*Clostridium*) *difficile*, despite cellular susceptibility to its toxins.  
867 *Anaerobe* 2019.
- 868 26. Mooyottu S, Flock G, Kollanoor-Johny A, Upadhyaya I, Jayarao B,  
869 Venkitanarayanan K. Characterization of a multidrug resistant *C. difficile* meat isolate.  
870 *IntJFood Microbiol* 2015; 192:111.
- 871 27. Aspinall ST, Hutchinson DN. New selective medium for isolating *Clostridium*  
872 *difficile* from faeces. *J Clin Pathol* 1992; 45:812-4.
- 873 28. Longo DL, Leffler DA, Lamont JT. *Clostridium difficile* Infection. *New England*  
874 *Journal of Medicine* 2015; 372:1539.
- 875 29. Kitahara M, Takamine F, Imamura T, Benno Y. *Clostridium hiranonis* sp. nov., a  
876 human intestinal bacterium with bile acid 7alpha-dehydroxylating activity.  
877 *IntJSystEvolMicrobiol* 2001; 51:39-44.
- 878 30. Fedorko DP, Williams EC. Use of cycloserine-cefoxitin-fructose agar and L-  
879 proline-aminopeptidase (PRO Discs) in the rapid identification of *Clostridium difficile*.  
880 *JClinMicrobiol* 1997; 35:1258.
- 881 31. Vital M, Rud T, Rath S, Pieper DH, Schluter D. Diversity of Bacteria Exhibiting  
882 Bile Acid-inducible 7 alpha-dehydroxylation Genes in the Human Gut. *Comput Struct*  
883 *Biotec* 2019; 17:1016-9.
- 884 32. Ridlon JM, Devendran S, Alves JM, Doden H, Wolf PG, Pereira GV, et al. The  
885 'in vivolifestyle' of bile acid 7 alpha-dehydroxylating bacteria: comparative genomics,  
886 metatranscriptomic, and bile acid metabolomics analysis of a defined microbial  
887 community in gnotobiotic mice. *Gut Microbes* 2020; 11:381-404.
- 888 33. Mullish BH, McDonald JAK, Pechlivanis A, Allegretti JR, Kao D, Barker GF, et  
889 al. Microbial bile salt hydrolases mediate the efficacy of faecal microbiota transplant in  
890 the treatment of recurrent. *Gut* 2019; 68:1791-800.
- 891 34. Stone NE, Nunnally AE, Roe CC, Hornstra HM, Wagner DM, Sahl JW. Complete  
892 Genome Sequence of Peptacetobacter (*Clostridium*) *hiranonis* Strain DGF055142,  
893 Isolated from Dog Feces from Flagstaff, Arizona, USA, 2019. *Microbiol Resour Announc*  
894 2021; 10.
- 895 35. Bochner BR. Global phenotypic characterization of bacteria. *FEMS*  
896 *MicrobiolRev* 2009; 33:191-205.

- 897 36. Scaria J, Chen JW, Useh N, He HX, McDonough SP, Mao CH, et al. Comparative  
898 nutritional and chemical phenotype of *Clostridium difficile* isolates determined using  
899 phenotype microarrays. International Journal of Infectious Diseases 2014; 27:20-5.
- 900 37. Nawrocki KL, Wetzel D, Jones JB, Woods EC, McBride SM. Ethanolamine is a  
901 valuable nutrient source that impacts *Clostridium difficile* pathogenesis. Environ  
902 Microbiol 2018; 20:1419-35.
- 903 38. Pitts AC, Tuck LR, Faulds-Pain A, Lewis RJ, Marles-Wright J. Structural insight  
904 into the *Clostridium difficile* ethanolamine utilisation microcompartment. PLoS One  
905 2012; 7:e48360.
- 906 39. Dawson LF, Donahue EH, Cartman ST, Barton RH, Bundy J, McNerney R, et al.  
907 The analysis of para-cresol production and tolerance in *Clostridium difficile* 027 and 012  
908 strains. BMC Microbiol 2011; 11:86.
- 909 40. Dawson LF, Stabler RA, Wren BW. Assessing the role of p-cresol tolerance in  
910 *Clostridium difficile*. J Med Microbiol 2008; 57:745-9.
- 911 41. Harrison MA, Faulds-Pain A, Kaur H, Dupuy B, Henriques AO, Martin-  
912 Verstraete I, et al. *Clostridioides difficile* para-Cresol Production Is Induced by the  
913 Precursor para-Hydroxyphenylacetate. JBacteriol 2020; 202.
- 914 42. Philipp B. Bacterial degradation of bile salts. Appl Microbiol Biot 2011; 89:903-  
915 15.
- 916 43. Studer N, Desharnais L, Beutler M, Brugiroux S, Terrazos MA, Menin L, et al.  
917 Functional Intestinal Bile Acid 7alpha-Dehydroxylation by *Clostridium scindens*  
918 Associated with Protection from *Clostridium difficile* Infection in a Gnotobiotic Mouse  
919 Model. Front Cell Infect Microbiol 2016; 6:191.
- 920 44. Kang JD, Myers CJ, Harris SC, Kakiyama G, Lee IK, Yun BS, et al. Bile Acid 7  
921 alpha-Dehydroxylating Gut Bacteria Secrete Antibiotics that Inhibit *Clostridium difficile*:  
922 Role of Secondary Bile Acids. Cell Chem Biol 2019; 26:27-+.
- 923 45. Winston JA, Theriot CM. Impact of microbial derived secondary bile acids on  
924 colonization resistance against *Clostridium difficile* in the gastrointestinal tract. Anaerobe  
925 2016; 41:44-50.
- 926 46. Wymore Brand M, Wannemuehler MJ, Phillips GJ, Proctor A, Overstreet AM,  
927 Jergens AE, et al. The Altered Schaedler Flora: Continued Applications of a Defined  
928 Murine Microbial Community. Ilar J 2015; 56:169-78.
- 929 47. Lyte JM, Proctor A, Phillips GJ, Lyte M, Wannemuehler M. Altered Schaedler  
930 flora mice: A defined microbiota animal model to study the microbiota-gut-brain axis.  
931 Behavioural Brain Research 2019; 356:221-6.
- 932 48. Wannemuehler MJ, Overstreet AM, Ward DV, Phillips GJ. Draft genome  
933 sequences of the altered schaedler flora, a defined bacterial community from gnotobiotic  
934 mice. Genome Announc 2014; 2.
- 935 49. Buffie CG, Bucci V, Stein RR, McKenney PT, Ling LL, Gobourne A, et al.  
936 Precision microbiome reconstitution restores bile acid mediated resistance to *Clostridium*  
937 *difficile*. Nature 2015; 517:205-U7.
- 938 50. Bastard QL, Ward T, Sidiropoulos D, Hillmann BM, Chun CL, Sadowsky MJ, et  
939 al. Fecal microbiota transplantation reverses antibiotic and chemotherapy-induced gut  
940 dysbiosis in mice. SciRep 2018; 8:6219.
- 941 51. Hand D, Wallis C, Colyer A, Penn CW. Pyrosequencing the canine faecal  
942 microbiota: breadth and depth of biodiversity. PLoS One 2013; 8:e53115.
- 943 52. Minamoto Y, Minamoto T, Isaiah A, Sattasathuchana P, Buono A, Rangachari  
944 VR, et al. Fecal short-chain fatty acid concentrations and dysbiosis in dogs with chronic  
945 enteropathy. J Vet Intern Med 2019; 33:1608-18.

- 946 53. AlShawaqfeh MK, Wajid B, Minamoto Y, Markel M, Lidbury JA, Steiner JM, et  
947 al. A dysbiosis index to assess microbial changes in fecal samples of dogs with chronic  
948 inflammatory enteropathy. *Fems Microbiology Ecology* 2017; 93.
- 949 54. Kaushik JK, Kumar A, Duary RK, Mohanty AK, Grover S, Batish VK. Functional  
950 and probiotic attributes of an indigenous isolate of *Lactobacillus plantarum*. *PLoS One*  
951 2009; 4:e8099.
- 952 55. Masuda N. Deconjugation of bile salts by Bacteroids and Clostridium. *Microbiol*  
953 *Immunol* 1981; 25:1-11.
- 954 56. Ridlon JM, Harris SC, Bhowmik S, Kang DJ, Hylemon PB. Consequences of bile  
955 salt biotransformations by intestinal bacteria. *Gut Microbes* 2016; 7:22-39.
- 956 57. Popoff MR, Bouvet P. Clostridial toxins. *Future Microbiol* 2009; 4:1021.
- 957 58. Bisht S, Singh KS, Choudhary R, Kumar S, Grover S, Mohanty AK, et al. Expression of fibronectin-binding protein of *L. acidophilus* NCFM and in vitro refolding  
958 to adhesion capable native-like protein from inclusion bodies. *Protein Expr Purif* 2018;  
959 145:7-13.
- 960 59. Styriak I, Zatkovic B, Marsalkova S. Binding of extracellular matrix proteins by  
961 lactobacilli. *Folia Microbiol (Praha)* 2001; 46:83-5.
- 962 60. Castaldo C, Vastano V, Siciliano RA, Candela M, Vici M, Muscariello L, et al. Surface displaced alfa-enolase of *Lactobacillus plantarum* is a fibronectin binding  
963 protein. *Microb Cell Fact* 2009; 8:14.
- 964 61. Identification and characterization of a fibronectin-binding protein from  
965 Clostridium difficile. *Microbiology*, 2003.
- 966 62. Shen W, Steinruck H, Ljungh A. Expression of binding of plasminogen,  
967 thrombospondin, vitronectin, and fibrinogen, and adhesive properties by *Escherichia coli*  
968 strains isolated from patients with colonic diseases. *Gut* 1995; 36:401-6.
- 969 63. Barketi-Klai A, Hoys S, Lambert-Bordes S, Collignon A, Kansau I. Role of  
970 fibronectin-binding protein A in Clostridium difficile intestinal colonization.  
971 *JMedMicrobiol* 2011; 60:1155.
- 972 64. Lin Y-P, Kuo C-J, Koleci X, McDonough S, Chang Y-F. Manganese Binds to  
973 Clostridium difficile Fbp68 and Is Essential for Fibronectin Binding. *Journal of*  
974 *Biological Chemistry* 2011; 286:3957.
- 975 65. Calabi E, Calabi F, Phillips AD, Fairweather NF. Binding of Clostridium difficile  
976 surface layer proteins to gastrointestinal tissues. *Infect Immun* 2002; 70:5770-8.
- 977 66. Passmore IJ, Letertre MPM, Preston MD, Bianconi I, Harrison MA, Nasher F, et  
978 al. Para-cresol production by Clostridium difficile affects microbial diversity and  
979 membrane integrity of Gram-negative bacteria. *PLoS Pathog* 2018; 14:e1007191.
- 980 67. Selmer T, Andrei PI. p-Hydroxyphenylacetate decarboxylase from Clostridium  
981 difficile. A novel glycol radical enzyme catalysing the formation of p-cresol. *Eur J*  
982 *Biochem* 2001; 268:1363-72.
- 983 68. Schulthess B, Brodner K, Bloomberg GV, Zbinden R, Bttger EC, Hombach M.  
984 Identification of Gram-Positive Cocci by Use of Matrix-Assisted Laser Desorption  
985 Ionization-Time of Flight Mass Spectrometry: Comparison of Different Preparation  
986 Methods and Implementation of a Practical Algorithm for Routine Diagnostics.  
987 *JClinMicrobiol* 2013; 51:1834-40.
- 988 69. Bolger AM, Lohse M, Usadel B. Trimmomatic: a flexible trimmer for Illumina  
989 sequence data. *Bioinformatics* 2014; 30:2114-20.
- 990 70. Wick RR, Judd LM, Gorrie CL, Holt KE. Unicycler: Resolving bacterial genome  
991 assemblies from short and long sequencing reads. *Plos Comput Biol* 2017; 13.
- 992
- 993

- 994 71. Walker BJ, Abeel T, Shea T, Priest M, Abouelliel A, Sakthikumar S, et al. Pilon:  
995 An Integrated Tool for Comprehensive Microbial Variant Detection and Genome  
996 Assembly Improvement. *PLoS One* 2014; 9.
- 997 72. Gurevich A, Saveliev V, Vyahhi N, Tesler G. QUAST: quality assessment tool  
998 for genome assemblies. *Bioinformatics* 2013; 29:1072-5.
- 999 73. Seemann T. Prokka: rapid prokaryotic genome annotation. *Bioinformatics* 2014;  
1000 30:2068-9.
- 1001 74. Eren AM, Esen OC, Quince C, Vineis JH, Morrison HG, Sogin ML, et al. Anvi'o:  
1002 an advanced analysis and visualization platform for 'omics data. *PeerJ* 2015; 3:e1319.
- 1003 75. Benedict MN, Henriksen JR, Metcalf WW, Whitaker RJ, Price ND. ITEP: An  
1004 integrated toolkit for exploration of microbial pan-genomes. *BMC Genomics* 2014; 15.
- 1005 76. Altschul SF, Gish W, Miller W, Myers EW, Lipman DJ. Basic Local Alignment  
1006 Search Tool. *J Mol Biol* 1990; 215:403-10.
- 1007 77. van Dongen S, Abreu-Goodger C. Using MCL to Extract Clusters from Networks.  
1008 *Methods Mol Biol* 2012; 804:281-95.
- 1009 78. Lin GL, Chai J, Yuan S, Mai C, Cai L, Murphy RW, et al. VennPainter: A Tool  
1010 for the Comparison and Identification of Candidate Genes Based on Venn Diagrams.  
1011 *PLoS One* 2016; 11.
- 1012 79. JA S, AL S. Inhibiting the initiation of *Clostridium difficile* spore germination  
1013 using analogs of chenodeoxycholic acid, a bile acid. *Journal of bacteriology* 2010; 192.
- 1014 80. MB F, CA A, R S, JA S. Bile acid recognition by the *Clostridium difficile*  
1015 germinant receptor, CspC, is important for establishing infection. *PLoS pathogens* 2013;  
1016 9.
- 1017 81. Mooyottu S, Kollanoor-Johny A, Flock G, Bouillaut L, Upadhyay A, Sonenshein  
1018 AL, et al. Carvacrol and trans-Cinnamaldehyde Reduce *Clostridium difficile* Toxin  
1019 Production and Cytotoxicity in Vitro. *IntJMolSci* 2014; 15:4415.
- 1020 82. F W, J F, N S, LC W, S B, A N, et al. RNAscope: a novel in situ RNA analysis  
1021 platform for formalin-fixed, paraffin-embedded tissues. *The Journal of molecular  
1022 diagnostics : JMD* 2012; 14.
- 1023 83. Littmann ER, Lee J-J, Denny JE, Alam Z, Maslanka JR, Zarin I, et al. Host  
1024 immunity modulates the efficacy of microbiota transplantation for treatment of  
1025 *Clostridioides difficile* infection. *Nature Communications* 2021; 12:1-15.
- 1026
- 1027

1028 **Table 1. Bacterial isolates recovered from 50 random canine fecal samples using**  
1029 **TMNF screening method.** The presence or absence of of *bai* and/or *bsh* genes known to  
1030 be present in the available genomes or literature for each bacterial isolate is listed.

1031

Bacteria	Isolation rate (%)	<i>bai</i> operon	<i>bsh</i> gene
<i>Bifidobacterium pseudolongum</i>	2	No	Yes
<i>C. bif fermentans</i>	4	Yes	Yes
<i>C. difficile</i>	6	No	No
<i>C. paraputreficum</i>	4	No	Yes
<i>C. sordelli</i>	2	Yes	No
<i>Eubacterium tenue</i>	2	No	Putative
<i>P. hiranonis</i>	4	Yes	Yes
<i>Parabacteroides distasonis</i>	2	No	Yes
<i>Terrisporobacter glycolicus</i>	2	No	No
<i>Clostridium sporogenes</i>	2	No	Yes

1032

1033 **Figures**

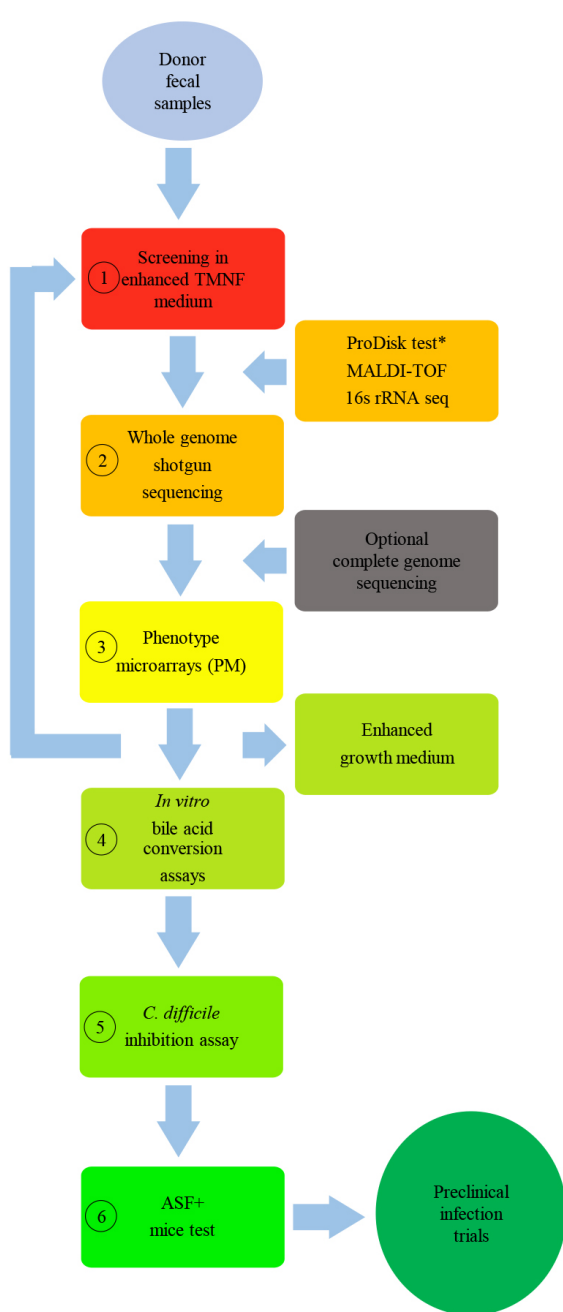
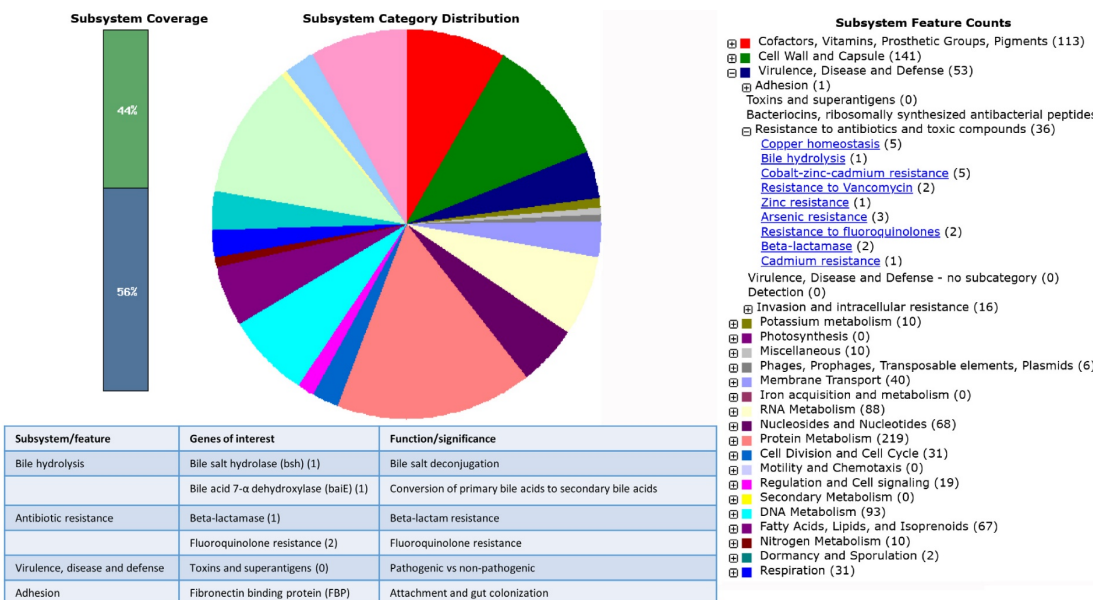


**Figure 1. Overview of the screening pipeline for *bai*-containing bacteria with anti-*C. difficile* biotherapeutic potential.** 1) screening in TMNF medium enables isolation of bile acid converting bacterium with similar growth condition as with *C. difficile*; 2) whole genome shotgun sequencing for identifying genes associated with bile acid transformation, virulence, antibiotic resistance and gut colonization; 3) Phenotype Microarrays (PM) allows formulation of specific screening media for specialized screening of a particular bacterium, preparation of an enhanced growth medium and predict the competitive substrate utilization of the candidate bacterium compared to *C. difficile*; 4) *in vitro* bile acid conjugation assay and 7- $\alpha$  dehydroxylation assay confirms and characterize the bile acid transformation ability of the candidate bacterium; 5) ASF<sup>+</sup> mice test confirms *in vivo* bile acid transformation and colonization ability of the candidate bacterium in the dysbiotic gut environment and assess the pathogenicity of the particular bacterium. \* ProDisk test, if included screens specifically *P. hiranonis*, *C. sordelli*, and *C. bif fermentans*

1052 *difficile*; 4) *in vitro* bile acid conjugation assay and 7- $\alpha$  dehydroxylation assay confirms  
1053 and characterize the bile acid transformation ability of the candidate bacterium; 5) ASF<sup>+</sup>  
1054 mice test confirms *in vivo* bile acid transformation and colonization ability of the candidate  
1055 bacterium in the dysbiotic gut environment and assess the pathogenicity of the particular  
1056 bacterium. \* ProDisk test, if included screens specifically *P. hiranonis*, *C. sordelli*, and  
1057 *C. bif fermentans*



1058 **Figure 2. Whole-genome shotgun sequencing of *P. hiranonis* BAI-17 reveals bile acid**

1059 **conversion genes and the absence of potential toxins and other virulence factors.** The

1060 bacterial DNA isolated from a pure culture of *P. hiranonis* BAI-17 was sequenced using

1061 the Illumina MiSeq platform. The assembled contigs were annotated using the RAST

1062 pipeline, and the genome and subsystems were visualized in Seed Viewer. The subsystem

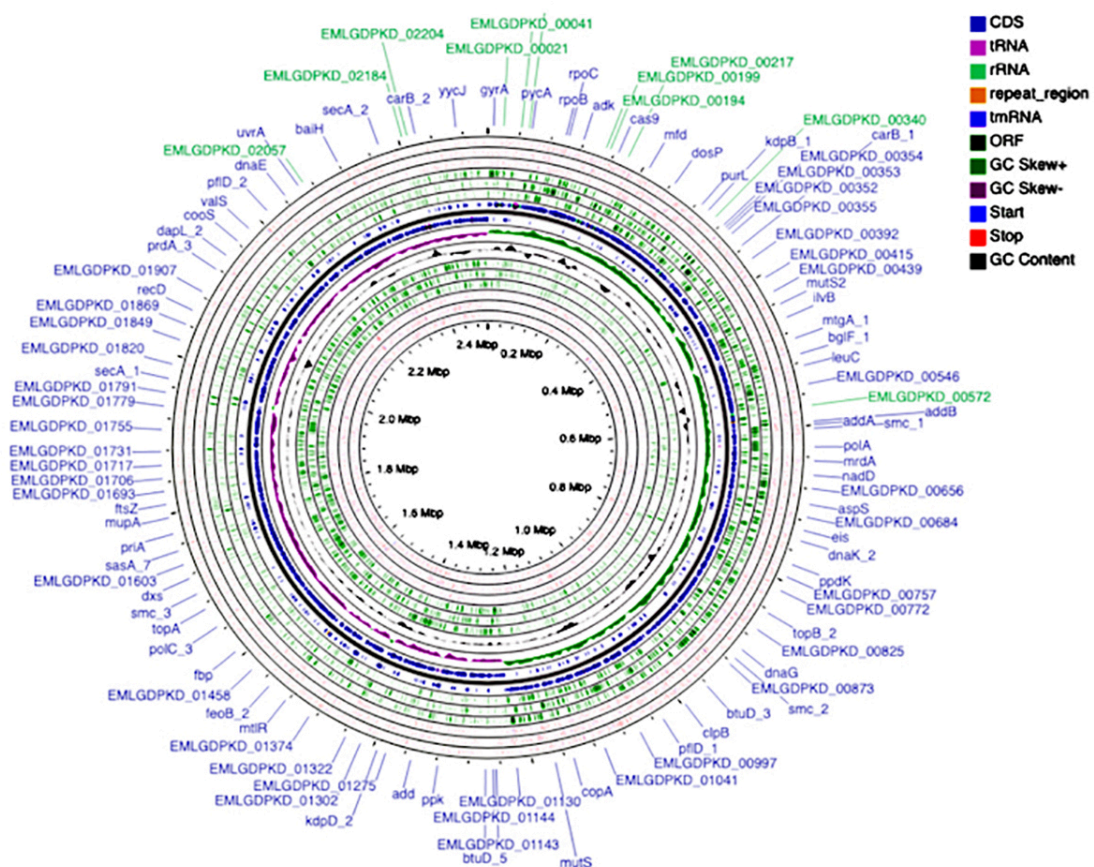
1063 category distribution and feature counts are depicted and listed on the right and left of the

1064 panel, respectively. The table summarizes the major *P. hiranonis* BAI-17 genes and

1065 functions that are favorable from an anti-*C. difficile* biotherapeutic perspective.

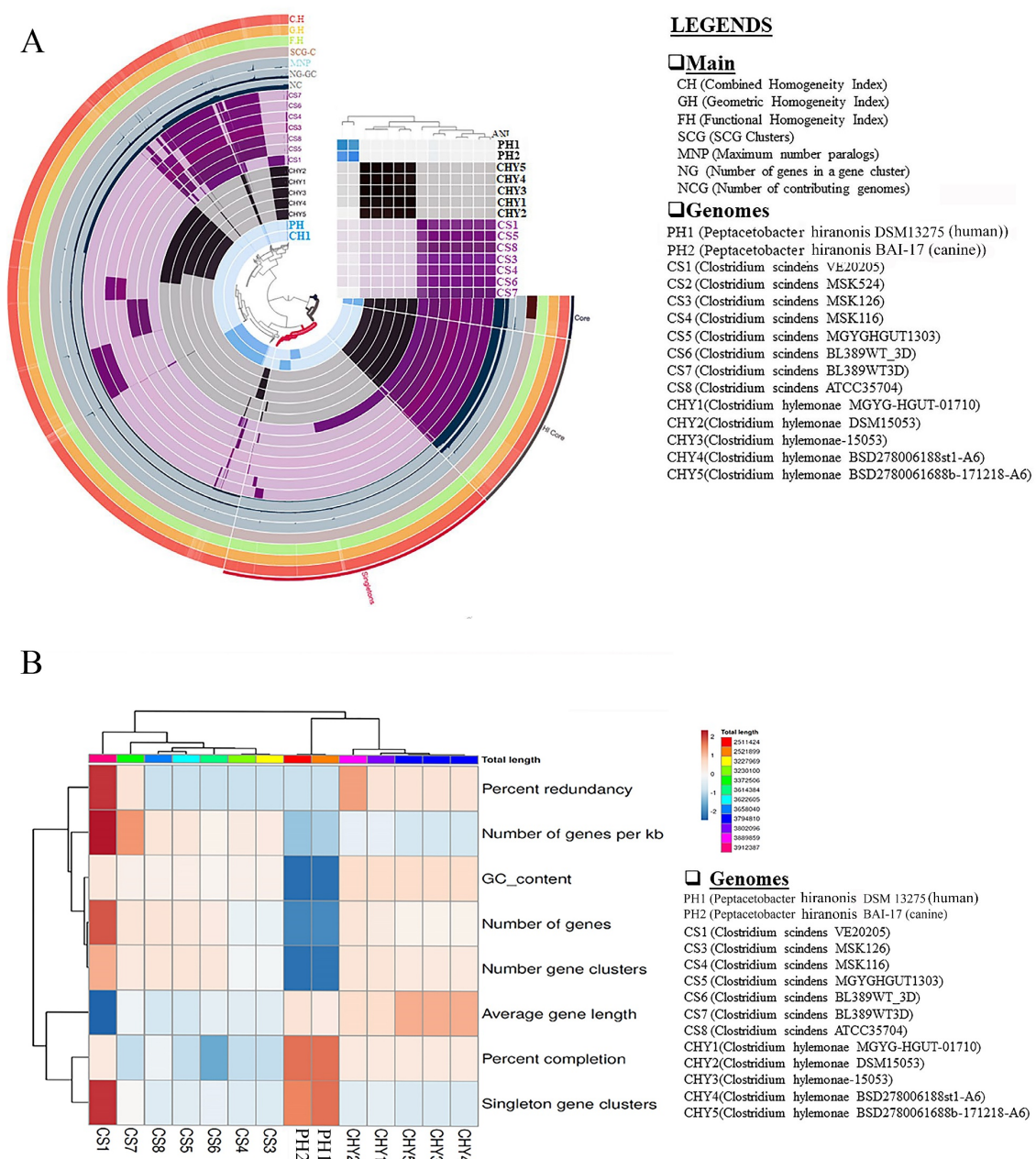
1066

1067



1068 **Figure 3. Circular complete genome plot for *P. hiranonis* BAI-17:** circular plot with  
1069 tracks showing the CDS, tRNA, rRNA, repeat\_region, tmRNA, ORF, GC Skew-, GC  
1070 Skew+, start codons, stop codons, and GC content.  
1071

1072



1073

1074 **Figure 4. Comparative pangenome analysis of *P. hiranonis BAI-17*: The Pangenome**

1075 analysis of *P. hiranonis BAI-17*, *P. (canine). hiranonis* DSM 13275 (human), seven *C.*

1076 *scindens* strains and four *C. hylemonae* strains (A) The genomic characteristics

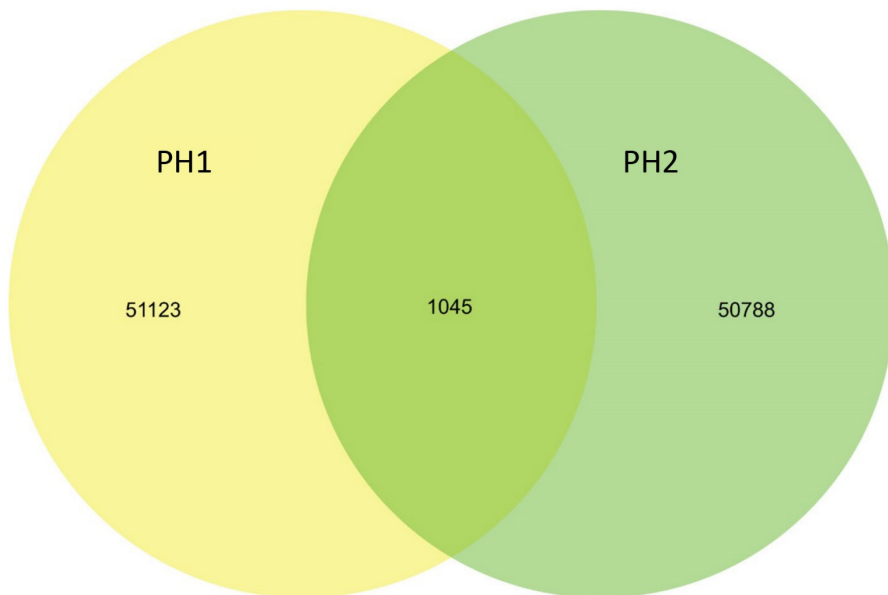
1077 highlighting the number of singleton gene clusters, average gene length, number of gene

1078 clusters, number of genes, GC\_ content, number of genes per kb, percentage redundancy

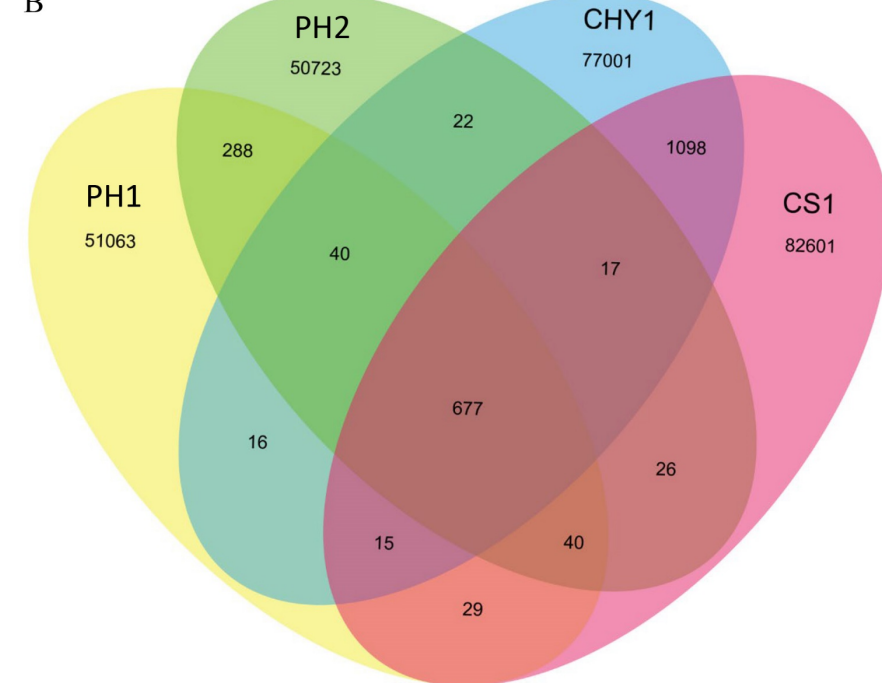
1079 and completion of each genome shown in a heatmap (B).

1080

A



B



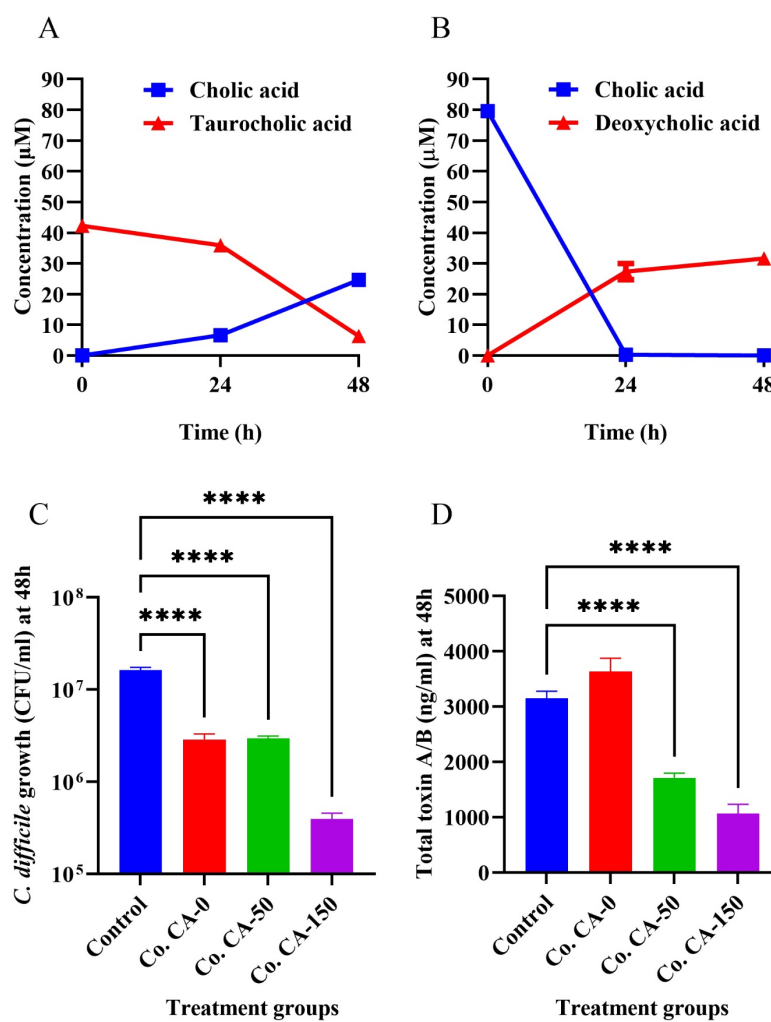
1081 **Figure 5. Comparative pangenome analysis of *P. hiranonis* BAI-15:** A) Comparative  
1082 analysis of gene families between canine origin *P. hiranonis* BAI17 and human origin *P.*  
1083 *hiranonis* DSM 1327; B) Gene family analysis of *P. hiranonis* BAI17 (PH2), *P. hiranonis*  
1084 DSM 13275 (PH1), *C. hylemonae* MGYG-HGUT-01710 (CHY1), and *C. scindens*  
1085 VE20205 (CS1) showing the number of unique, shared and core genes within the  
1086 genomes.

PM Plate ID	Substrate	% Growth increase*
A1	Negative control	0
<b>Carbon Sources</b>		
PM1- G1	Glycyl-L-Glutamic Acid	64.58
PM1- E1	L-Glutamine	52.35
PM1- H12	2-Aminoethanol	47.29
PM1- H2	p-Hydroxy Phenyl Acetic	47.03
PM1- G12	L-Malic Acid	45.6
PM1- H3	m-Hydroxy Phenyl Acetic	44.04
PM1- F1	Glycyl-L-Aspartic Acid	41.86
PM1- H1	Glycyl-L-Proline	41.43
PM1- H5	D-Psicose	37.49
PM1- D1	L-Asparagine	36.66
PM1- H7	Glucuronamide	36.53
PM1- H4	Tyramine	36.07
PM1- E12	Adenosine	34.63
PM1- H10	D-Galacturonic Acid	33.39
PM1- H8	Pyruvic acid	33.38
PM1- E11	2-Deoxy Adenosine	33.31
PM1- H9	L-Galactonic Acid- $\gamma$ -Lactone	33.24
PM1- H6	L-Lyxose	31.91
PM1- A3	N-Acetyl-D-Glucosamine	28.81
PM1- H11	Phenylethylamine	28.41
PM1- G11	D-Malic Acid	26.91
PM1- A6	D-Galactose	26.39
PM1- C7	D-Fructose	25.04
PM1- C9	$\alpha$ -D-Glucose	23.91
PM1- E10	Maltotriose	23.86
PM1- D11	Sucrose	23.72
PM1- G2	Triearballyc Acid	23.66
PM1- A11	D-Mannose	21.17
<b>Carbon Sources</b>		
PM2A- H3	L-Pyroglutamic Acid	54.31
PM2A- H6	Sec-Butylamine	49.62
PM2A- H12	3-Hydroxy-2-Butanone	49.09
PM2A- H7	D,L-Octopamine	49.05
PM2A- H5	D,L-Camitine	48.46
PM2A- H4	L-Valine	46.58
PM2A- G2	L-Alanamide	42.56
PM2A- H1	L-Ornithine	42.44
PM2A- G12	L-Methionine	40.42
PM2A- G1	Acetamide	40.35
PM2A- H9	Dihydroxy Acetone	37.45
PM2A- E12	5-Keto-D-Gluconic Acid	34.52
PM2A- H8	Putrescine	31.31
PM2A- H10	2,3-Butanediol	30
PM2A- F1	D-Lactic Acid Methyl Ester	26.97
PM2A- H2	L-Phenylanine	26.22
PM2A- G11	L-Lysine	25.22
PM2A- C2	L-Glucose	24.65
PM2A- H11	2,3-Butanedione	24.59
PM2A- G3	N-Acetyl-L-Glutamic Acid	24.04
PM2A- G4	L-Arginine	23.2
PM2A- D1	D-Raffinose	20.72
<b>Nitrogen Sources</b>		
PM3B- G10	D,L- $\alpha$ -Amino-Caprylic Acid	49.7
PM3B- H2	Ala-Gln	49.03
PM3B- H1	Ala-Asp	38.46
PM3B- B1	L-Glutamine	36.38
PM3B- H12	Met-Ala	31.89
PM3B- E1	Histamine	30.64
PM3B- H3	Ala-Glu	28.78
PM3B- H6	Ala-Leu	24.42
PM3B- G1	Xanthine	23.81
PM3B- H9	Gly-Gln	23.59
PM3B- H10	Gly-Glu	22.16
<b>Phosphorus and Sulfur sources</b>		
PM4A- E1	O-Phospho-D-Tyrosine	40.41
PM4A- D1	D-Mannose-1-Phosphate	27.39
PM4A- H2	Thiourea	21.98
<b>Nutrient Supplements</b>		
PM5- B1	L-Glutamine	38.72
PM5- E12	2'-Deoxy Uridine	32.95
PM5- H8	Choline	30.64
PM5- G12	myo-Inositol	30.37
PM5- H6	D,L-Mevalonic Acid	29.09
PM5- D8	D-Glutamic Acid	27.82
PM5- H3	$\alpha$ -Keto-Butyric Acid	27.63
PM5- D7	D-Aspartic Acid	27.38
PM5- E11	Uridine	26.96
PM5- H4	Caprylic Acid	25.97
PM5- E1	Putrescine	25.01
PM5- D9	D,L- $\alpha$ , $\epsilon$ -Diaminopimelic Acid	24.58
PM5- E10	Uracil	23.84
PM5- G11	Menadionine	22.99
PM5- D12	2'-Deoxy Cytidine	22.31
PM5- G9	Riboflavin	21.88
PM5- H7	D,L-Camitine	21.66
PM5- H2	D,L- $\alpha$ -Hydroxy-Butyric Acid	21.56
PM5- D1	L-Ornithine	21.38
PM5- H1	Butyric acid	21.26
<b>Peptide Nitrogen Sources</b>		
PM6- E1	Glu-Val	55.28
PM6- G1	His-Tyr	55.24
PM6- H2	Ile-Tyr	49.65
PM6- H9	Leu-Ile	44.08
PM6- H1	Ile-Trp	43.89
PM6- D1	Asp-Phe	43.28
PM6- H12	Leu-Phe	41.12
PM6- H6	Leu-Asp	40.9
PM6- H3	Ile-Val	39.57
PM6- A2	L-Glutamine	36.81
PM6- H4	Leu-Ala	35.77
PM6- H8	Leu-Gly	35.67
PM6- G12	Ile-Ser	34.84
PM6- H11	Leu-Met	33.82
PM6- H7	Leu-Glu	29.62
PM6- G2	His-Val	29.61
PM6- F1	Gly-Thr	26.21
PM6- H10	Leu-Leu	22.88
PM6- D12	Glu-Tyr	22.46
<b>Peptide Nitrogen Sources</b>		
PM7- H12	$\gamma$ -Glu-Gly	52.89
PM7- H1	Tyr-Tnp	45.12
PM7- H2	Tyr-Tyr	35.64
PM7- H9	Val-Leu	34.22
PM7- G12	Tyr-Phe	31.61
PM7- H6	Val-Gly	31.33
PM7- H3	Val-Arg	31.01
PM7- H11	Val-Val	30.99
PM7- A2	L-Glutamine	30.58
PM7- H5	Val-Asp	26.97
PM7- H4	Val-Asn	26.13
PM7- D12	Pro-Tyr	22.98
PM7- H8	Val-Ile	21.15
PM7- H7	Val-His	20.95
<b>Peptide Nitrogen Sources</b>		
PM8- H2	Gly-Gly-D-Leu	30
PM8- A2	L-Glutamine	22.35
PM8- H3	Gly-Gly-Gly	22.17

\* % increase in growth compared to negative control normalized to 1

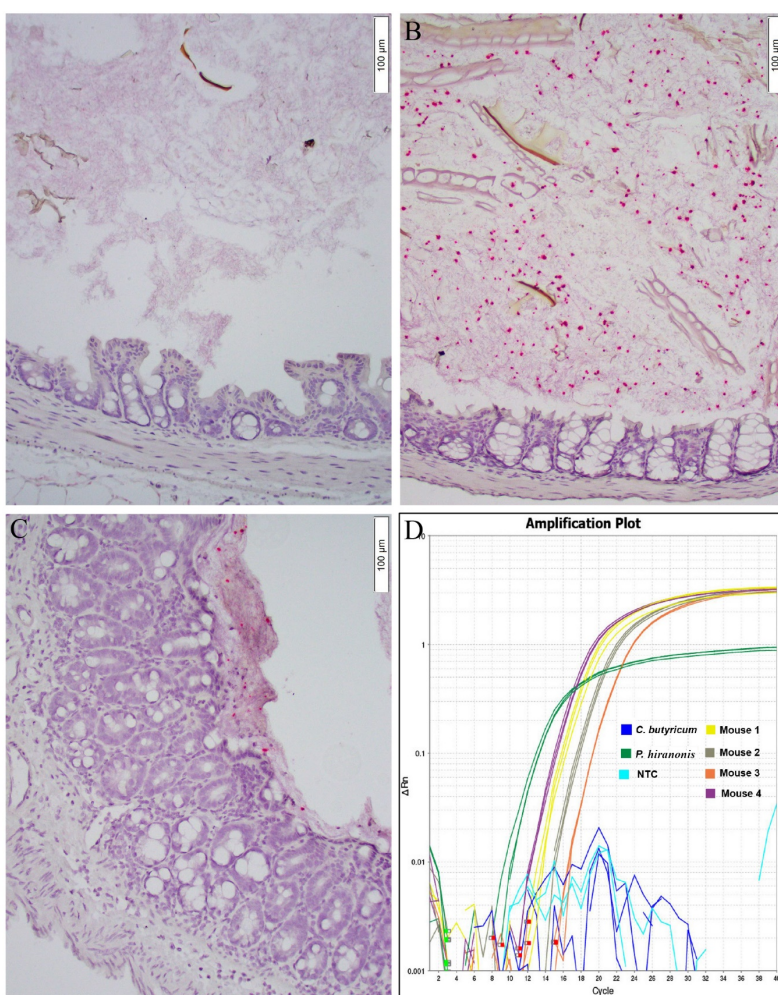
1087 **Figure 6. Substrate utilization of *P. hiranonis* BAI-17 in Biolog Phenotype**

1088 **Microarrays:** The nutritional phenotype of *P. hiranonis* BAI-17 strain was determined  
 1089 using Biolog Phenotype MicroArray panels 1–8. Each row represents a nutritional  
 1090 phenotype that increased the bacterial growth by at least 20% of the negative control (i.e.,  
 1091 bacterial growth equivalent to 120% of the negative control). The nutrient utilization for  
 1092 each panel is represented as a heat map in descending order of % increase in growth  
 1093 compared to the negative control (E.g., 169% of negative control means' 69% increase in  
 1094 growth').



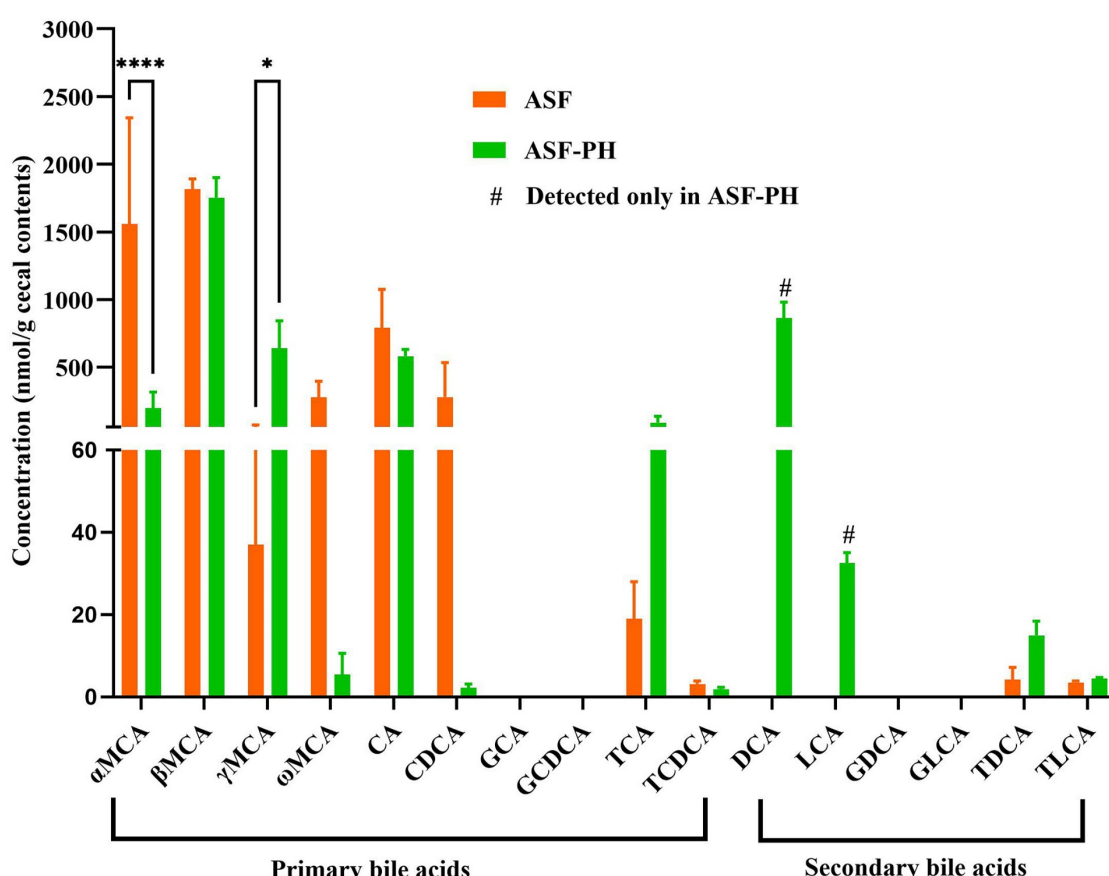
1095 **Figure 7. *P. hiranonis* BAI-17 exhibits robust bile acid deconjugation (A) and 7- $\alpha$   
1096 dihydroxylation (B) ability and inhibits *C. difficile* growth *in vitro*: A) *P. hiranonis*  
1097 *BAI-17* was cultured anaerobically in supplemented brain heart infusion (BHIS) broth  
1098 with 50 $\mu$ M taurocholic acid, and the bile acids were quantitated from culture supernatants  
1099 at 0, 24, and 48h using LC/MS technique. Taurocholate was completely deconjugated to  
1100 cholic acid within 48h. B) *P. hiranonis* BAI-17 was cultured anaerobically in  
1101 supplemented brain heart infusion (BHIS) broth with 100 $\mu$ M cholic acid, and the bile  
1102 acids were quantitated from culture supernatants at 0, 24, and 48h using LC/MS  
1103 technique. Cholic acid was completely depleted to secondary bile acid DCA and other  
1104 unmeasured metabolites by 24h; n=6 per experiment. C) *C. difficile* UK1 and *P. hiranonis*  
1105 BAI-17 (10 $^5$  CFU/ml inoculum each) were cocultured anaerobically in BHIS broth with**

1106 0, 50, or 150 $\mu$ M cholic acid separately (n=6). *C. difficile* count at 48h was determined by  
1107 anaerobic dilution and plating on blood agar supplemented with taurocholate. The Control  
1108 group (blue bar) represents the growth of *C. difficile* alone. **D)** 48h culture supernatant  
1109 from the coculture broth was assayed for total toxin A and B using quantitative ELISA.  
1110 Groups: *C. difficile* alone (no coculture) (Control); *C. difficile* and *P. hiranonis* coculture  
1111 with no i.e.. 0 $\mu$ M cholic acid (Co. CA-0); coculture with 50 $\mu$ M cholic acid (Co. CA-50);  
1112 and coculture with 150 $\mu$ M cholic acid (Co. CA-150). \*\*\*p<0.0001  
1113



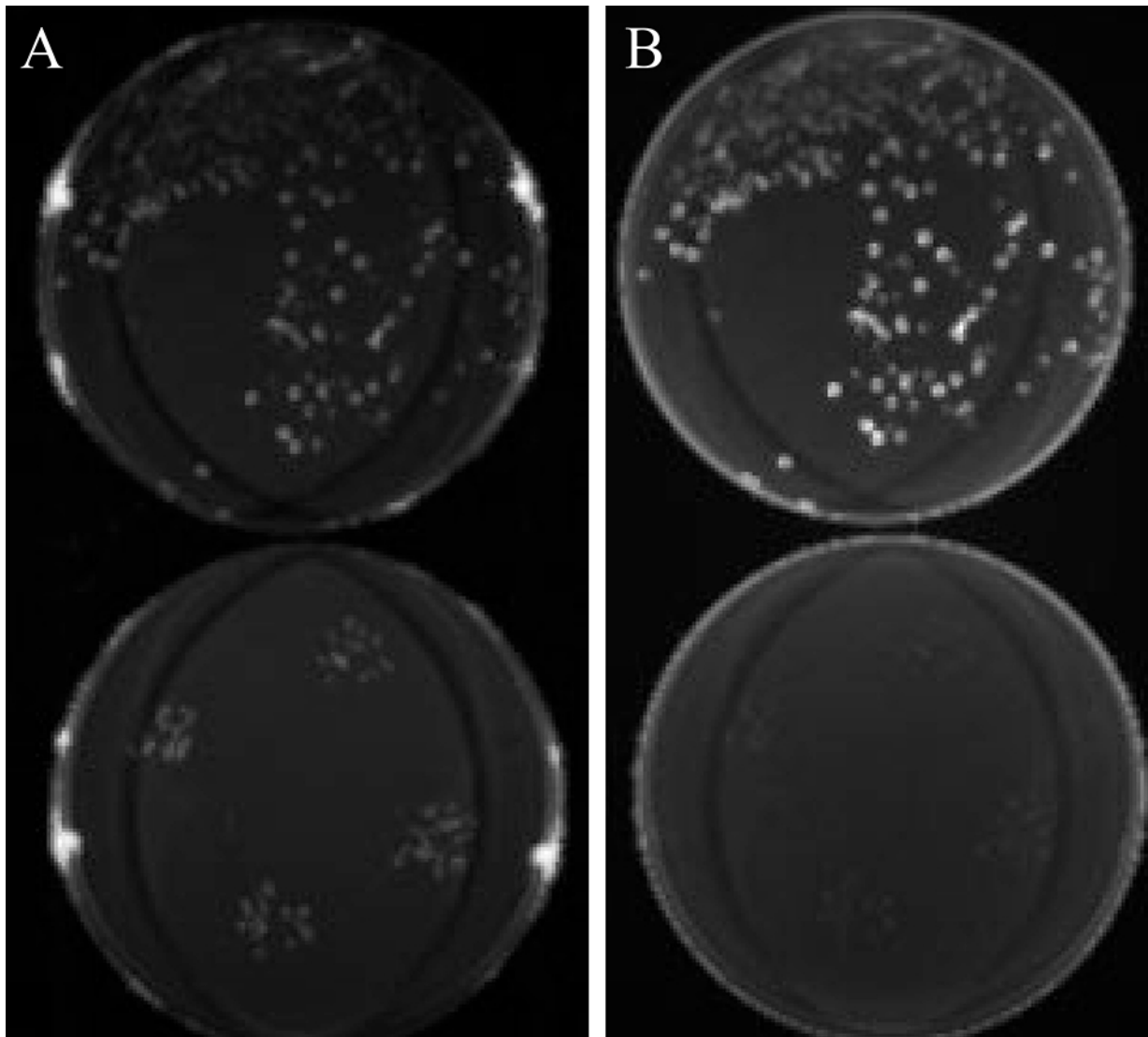
1114 **Figure 8. *P. hiranonis* BAI-17 colonizes ASF mice:** Six-week-old ASF mice were  
1115 inoculated via single oral gavage with 250  $\mu$ l of  $10^5$  CFU/mL *P. hiranonis* BAI-17 or  
1116 PBS. The animals were euthanized, and the large intestine with contents were collected  
1117 after 3-week post-inoculation. *P. hiranonis* BAI-17 bacteria (red signal) was demonstrated  
1118 by RNAscope *in situ* hybridization technique using custom-made specific RNAscope  
1119 probes. (A): cecum-negative control (ASF); B): cecal luminal contents of an ASF mouse  
1120 colonized with *P. hiranonis* BAI-17; C): depiction of tight mucus in the colon an ASF  
1121 mouse colonized with *P. hiranonis* BAI-17 **D)** Colonization with *P. hiranonis* BAI-17  
1122 was initially confirmed by TaqMan based qPCR using fresh fecal pellets collected from  
1123 individual mice three weeks post-inoculation (result from four ASF shown). DNA from  
1124 *P. hiranonis* BAI-17 and *Clostridium butyricum*, along with a non-template control (NTC)  
1125 were included as test controls.

1126



1127 **Figure 9.  $ASF^+$  test demonstrates the formation of secondary bile acids in the cecal  
1128 contents from  $ASF$  mice colonized with *P. hiranonis* BAI-17 (ASF-PH) but not in  
1129  $ASF$  control mice:** Six-week-old  $ASF$  mice ( $n=6$ ) were inoculated with single oral  
1130 gavage with  $250 \mu\text{l}$  of  $10^5$  *P. hiranonis* BAI-17 to generate  $ASF$ -PH mice. Cecal contents  
1131 from both  $ASF$ -PH mice and age-matched control  $ASF$  mice were quantified for primary  
1132 and secondary bile acids using targeted metabolomics analysis. Primary bile acids: MCA:  
1133 muricholic acid; CA: cholic acid; CDCA: chenodeoxyxholic acid; GCA: glycocholic  
1134 acid; GCDCA: glycochededeoxyxholic acid; TCA: taurococholic acid; TCDCA:  
1135 taurochdedeoxyxholic acid. Secondary bile acids: DCA deoxycholic acid; LCA;  
1136 lithocholic acid; GDCA glycodeoxycholic acid; GLCA; glycolithocholic acid; TDCA  
1137 taurodeoxycholic acid; TLCA; taurolithocholic acid. # detected only in  $ASF$ -PH but not  
1138 in  $ASF$  control mice; \*\*  $p < 0.005$ ; \*\*\*\*  $p < 0.0001$ .

1139 **Supplementary data:**



1140 **Supplementary figure 1: Fluorescence under ultraviolet (UV-6) discriminates *C.***  
1141 ***difficile* colonies from *P. hiranonis* colonies on blood agar.** *C. difficile* UK1 (petri dish  
1142 on the top in panels A and B) and *P. hiranonis* BAI-17 (petri dish on the bottom in panels  
1143 A and B) were cultured on blood agar and incubated in anaerobic conditions for 48 h at  
1144 37°C. The colonies were visualized under visible light (panel A) and UV-6 (panel B)  
1145 using a G BOX chemi XRQ UV transilluminator (Syngene, Frederick, MD). *C. difficile*  
1146 colonies were brightly illuminated (top petri dish, panel B) under UV, while *P. hiranonis*  
1147 colonies were illuminated only under visible light (bottom petri dish, panel B).

1148

Bacteria	Isolation rate (%)
<i>C. baratii</i>	0.37
<i>C. boltae</i>	0.37
<i>C. butyricum</i>	0.37
<i>C. celerecrescens</i>	0.74
<i>C. cochlearium</i>	2.59
<i>C. colicanis</i>	0.37
<i>C. difficile</i>	23.70
<i>C. innocum</i>	1.85
<i>C. paraputrificum</i>	2.22
<i>C. perferingens</i>	2.59
<i>C. ramosum</i>	0.37
<i>C. sordelli</i> *	0.37
<i>C. sphenoides</i>	0.74
<i>C. sporogenes</i>	5.93
<i>C. tertium</i>	4.07
<i>P. bif fermentans</i> *	4.44
<i>T. glycolicus</i>	4.44

1149

1150 **Supplementary Table 1. Bacterial species isolated from 270 random canine fecal**  
1151 **samples using CCFA medium.** Two seventy random canine fecal samples were enriched  
1152 in BHIS medium in anaerobic conditions for 48 h at 37°C for seven days, followed by  
1153 three days of oxygen shock. 1 ml of the media was centrifuged, the pellet was alcohol  
1154 shocked with 100% ethanol for 20 minutes and plated on a CCFA agar plate  
1155 supplemented with 0.1% taurocholate. The identity of Pro DISK positive colonies was

1156 confirmed by MALDI-TOF and 16s rRNA sequencing. \* Indicates *bai*-containing

1157 bacteria.

1158

1159